ISSN: 2165-3259

JAOCR

Official Journal of the American Osteopathic College of Radiology

NEUROIMAGING

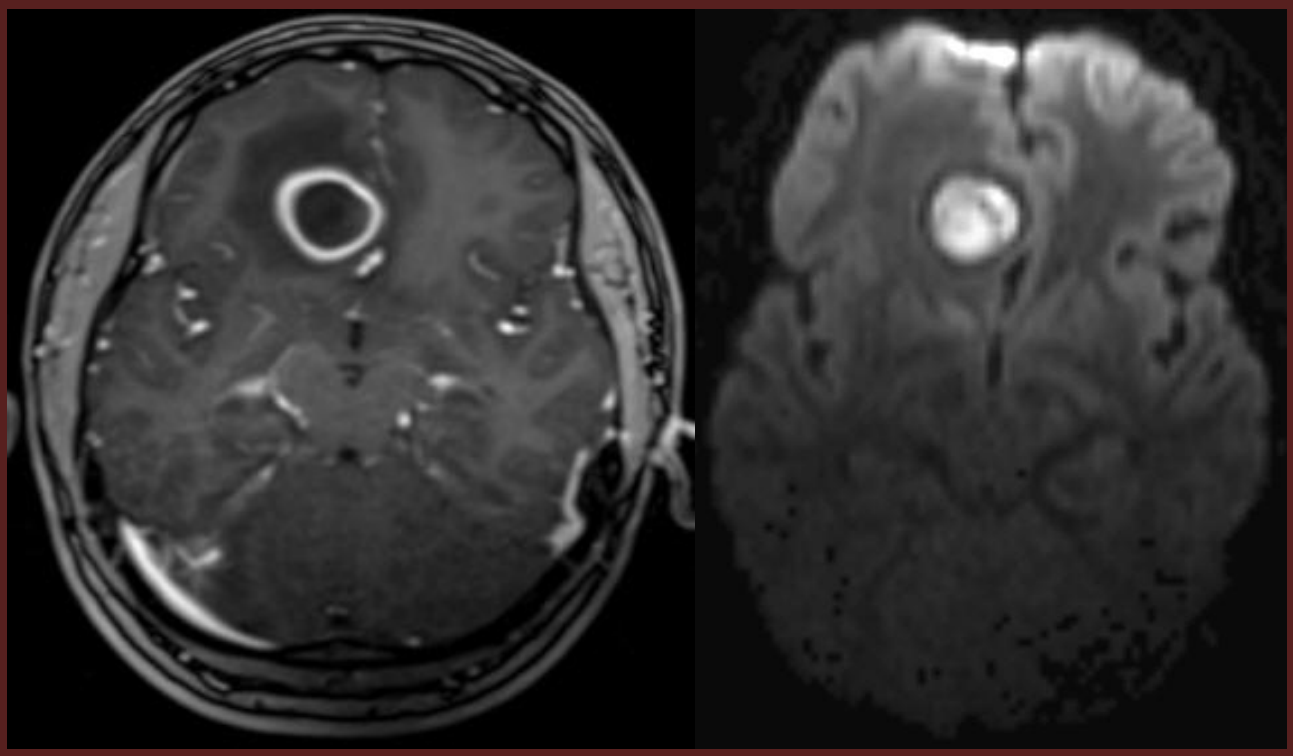

January 2012, Vol. 1, Issue 1

JAOCR
Official Journal of the American Osteopathic College of Radiology

Aims and Scope

The *Journal of the American Osteopathic College of Radiology* (*JAOCR*) is designed to provide practical up-to-date reviews of critical topics in radiology for practicing radiologists and radiology trainees. Each quarterly issue covers a particular radiology subspecialty and is composed of high quality review articles and case reports that highlight differential diagnoses and important teaching points.

Access to Articles

All articles published in the *JAOCR* are open access online. Subscriptions to the journal are not required to view or download articles. Reprints are not available.

Copyrights

Guide for Authors

Submissions for the *JAOCR* are by invitation only. If you were invited to submit an article and have questions regarding the content or format, please contact the appropriate Guest Editor for that particular issue. Although contributions are invited, they are subject to peer review and final acceptance.

Editor-in-Chief

Design Editor

Editorial Committee

Neuroimaging

Editor: William T. O'Brien, Sr., D.O.

Letter from the President

George E. Erbacher, D.O., F.A.O.C.R.

President, *American Osteopathic College of Radiology*

"As our case is new, so we must think anew, and act anew."

Abraham Lincoln

Welcome to the inaugural issue of the Journal of the American Osteopathic College of Radiology (JAOCR).

The Journal is the brain child of AOCR member, Dr. William T. O'Brien, Sr., DO., who has extensive experience as a researcher and author including textbooks and book chapters.

When Dr. O'Brien approached the AOCR Board of Directors with the idea for the JAOCR, the concept was embraced whole-heartedly as he agreed to be editor and guide us. Because of his extensive experience, the path to this inaugural issue has been rapid. Many AOCR members have research and publishing experience, and to be able to share practical knowledge with our members and members in training is exciting. The goal is not to duplicate what already exists in the imaging journal world but to focus on information that is applicable to our everyday practices. See the "From the Editor" page in this journal.

To be able to be on the forefront of supporting our members is the goal. We invite all members to give us feedback via email/mail, etc., to help make this journal fit their needs.

Huge thanks are due to Dr. Frederick White (President-elect and Chair of the Editorial Committee) for spear-heading and encouraging this effort. As always, the AOCR staff has done all the work behind the scenes, especially Communications Director, Ms. Jessica Roberts, who manages the JAOCR website and provides communication between the many AOCR committees and the many AOCR members. Pam Smith, Executive Director, because of her long-dedicated experience with the AOCR and relationships with our members has put us in contact with contributors. Pam also, as Executive Director, has kept us fiscally responsible in this endeavor.

Enjoy this inaugural JAOCR. You are encouraged to be a contributor. Please text/tweet/email, etc., Jessica. Let us know your thoughts on how to shape this journal for your needs.

We at the AOCR are excited to bring you this journal, and we want you to be equally excited as we take this giant leap in serving our member's educational needs.

In this Issue

William T. O'Brien, Sr., D.O.

Editor-in-Chief, *Journal of the American Osteopathic College of Radiology*

"I refuse to join any club that would have me as a member."

Groucho Marx

It is a tremendous honor to present the inaugural issue of the *Journal of the American Osteopathic College of Radiology* (*JAOCR*). The goal of the Journal is to produce a high quality educational resource for the AOCR and its members.

The Journal will be published quarterly as an online, open access journal with each issue covering a single radiology subspecialty. Each issue will include 2-3 review articles, case reports, and interesting images with a caption in a section referred to as "*JAOCR* At the Viewbox." Guest editors will be invited for each issue. They will recruit experts in their respective fields to author articles for the Journal. We hope that the end result will be an exceptional resource geared towards general radiologists and radiology trainees.

I would like to thank the AOCR leadership and staff for their support in establishing the *JAOCR*. I especially would like to thank Drs. George Erbacher, President, and Frederick White, President-elect, for being major proponents of this project from its onset. Ms. Jessica Roberts, Communications Director, has been invaluable in developing and managing the *JAOCR* website, as well as coordinating and routing the numerous proposals and nominations through the AOCR committees. Pamela Smith, Executive Director, has been instrumental in recommending and contacting contributors and providing valuable insight into the overall management of the Journal.

This first issue covers the field of neuroradiology, which is near and dear to my heart as it is my field of subspecialty training. We have superb review articles from world-renowned experts covering CNS vascular malformations (Alice Boyd Smith, M.D., American Institute for Radiologic Pathology) and CNS manifestations of non-accidental trauma (Gary Hedlund, D.O., Primary Children's Medical Center in Salt Lake City, Utah). The case report section of the Journal introduces a unique high-yield format with cases involving head and neck and spine imaging. The final section, "*JAOCR* At the Viewbox," includes images from interesting cases with short captions.

In order to establish format templates for this and subsequent issues, I participated in authoring one article in each of the three sections of the Journal, including a review article on imaging of CNS infections in immunocompetent hosts. In future issues, my role will primarily be editorial in support of the guest editors to help ensure the highest quality content for the Journal.

I hope that you enjoy this inaugural issue. Given the talent and expertise within the AOCR, I hope that this will just be the beginning of a long and successful run for the *JAOCR*.

The views expressed in this material are those of the author, and do not reflect the official policy or position of the U.S. Government, the Department of Defense, or the Department of the Air Force.

Imaging of CNS Infections in Immunocompetent Hosts

William T. O'Brien, Sr., D.O.

Division of Neuroradiology, Wilford Hall Ambulatory Surgical Center, San Antonio, TX

Infections of the central nervous system (CNS) are an important cause of morbidity and mortality in immunocompetent hosts. Common etiologies include bacterial, viral, and parasitic infections, some of which are ubiquitous, while others primarily occur within endemic regions. Clinical presentations vary based upon the age of the patient and nature of the infection. Imaging manifestations mirror the portions of the brain which are affected, whether it be the brain parenchyma or its overlying protective meningeal coverings. At times, the imaging patterns suggest the causative agent. Knowledge of the common imaging patterns and potential complications of CNS infections is critical in prompt and accurate diagnosis and treatment, which will in turn minimize adverse outcomes.

Meningitis

Meningitis refers to inflammation involving the protective meningeal coverings of the brain. It is the most common form of CNS infection. Most cases result from hematogenous spread of an infection from a distant site. Other etiologies include direct spread from sinonasal or mastoid infections, extension of cortical abscesses, postsurgical complications, or penetrating trauma. The infectious and inflammatory exudates infiltrate and spread along the meninges and perivascular spaces.

The responsible organisms and clinical presentations vary based upon the age of the patient. Viral infections are more common than bacterial; however, bacterial infections are more prone to serious illness and complications. Meningitis remains a clinical diagnosis with confirmation by lumbar puncture. Imaging is generally reserved for cases in which the diagnosis is unclear, to evaluate for potential complications, or if the patient experiences clinical deterioration, seizures, or focal neurological deficits.

In neonates, meningitis is most often acquired during childbirth or as a result of chorioamnionitis. There is an increased risk with prematurity and prolonged rupture of membranes. *Group B Streptococcus*, *Escherichia coli*, and *Listeria monocytogenes* are the most common organisms. Clinical presentation is nonspecific, often resulting in irritability, sepsis, and occasionally seizures. In older children and adults, *Streptococcus pneumoniae*, *Haemophilus influenza*, and *Neisseria meningitidis* are the most common organisms. *Neisseria* is especially prevalent in dormitory settings. Fever, headache, and nuchal rigidity are the most common clinical presentations in these patients.

Imaging in the setting of uncomplicated meningitis is most often normal. Magnetic resonance imaging (MRI) is more sensitive than computed tomography (CT) in evaluating for meningeal disease.[1] Early in the disease process, MRI may show increased FLAIR signal intensity within the subarachnoid space[2] (Fig. 1) with or without abnormal meningeal enhancement. Leptomeningeal enhancement (Fig. 2) may be smooth or nodular and is more common than pachymeningeal (dural) enhancement (Fig. 3). In general, most bacterial infections involve the cerebral convexities, while atypical infections (*Mycobacterium tuberculosis* and fungal infections) preferentially involve the skull base and basal cisterns.

Complications of meningitis include hydrocephalus, ventriculitis, venous thrombosis, subdural empyema, and extension into the underlying brain parenchyma with cerebritis or abscess formation.[3] Hydrocephalus can be categorized as communicating (extraventricular obstructive hydrocephalus) or noncommunicating (intraventricular obstructive hydrocephalus). Communicating hydrocephalus is more common and results from inflammatory exudates interfering with resorption of cerebrospinal fluid (CSF) at the

arachnoid villi. Noncommunicating hydrocephalus may occur at the cerebral aqueduct or fourth ventricular outlet foramina as a result of inflammatory webs or adhesions. Acute, uncompensated hydrocephalus results in increased intraventricular pressure with associated transependymal flow of CSF, which manifests as a rind of increased T2/FLAIR signal intensity along the margins of the lateral ventricles (Fig. 4).

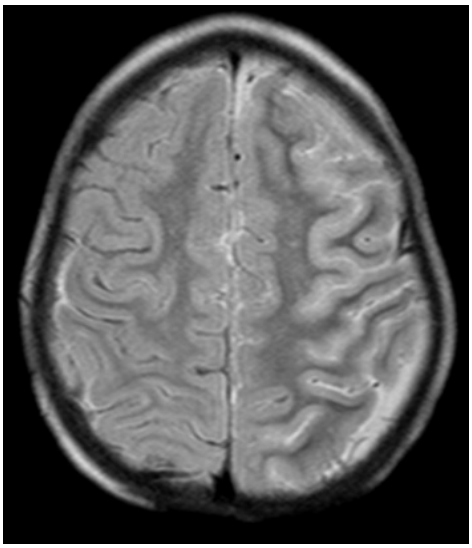

Figure 1. Meningitis. Axial FLAIR image demonstrates increased signal intensity involving the subarachnoid spaces overlying the left greater than right cerebral hemispheres. There is also abnormal signal and edema within the underlying gyri.

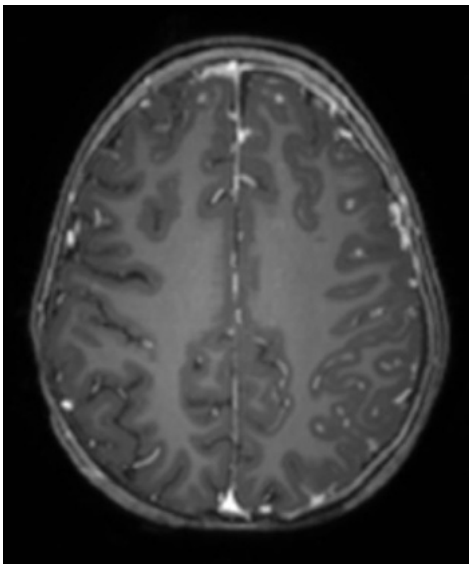

Figure 2. Leptomeningeal enhancement. Axial T1 post contrast image with fat suppression reveals nodular leptomeningeal enhancement overlying the left cerebral hemisphere and right frontal lobe.

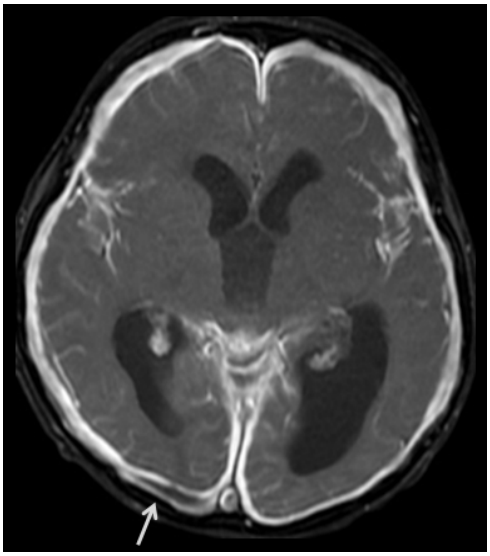

Figure 3. Pachymeningeal enhancement. Axial T1 post contrast image with fat suppression demonstrates diffuse thick pachymeningeal enhancement overlying both cerebral hemispheres. There are also regions of underlying leptomeningeal enhancement and an epidural abscess superficial to the right occipital lobe (arrow).

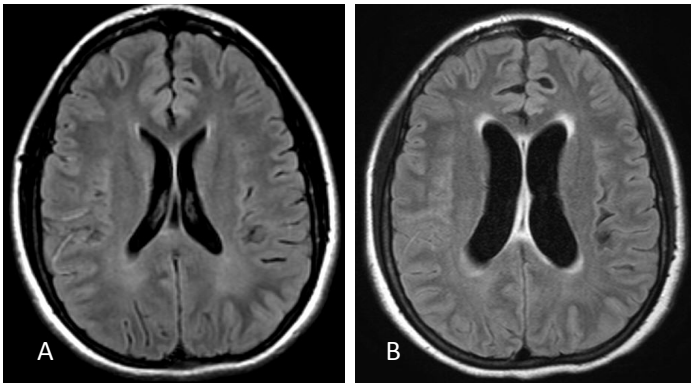

Figure 4. Hydrocephalus. Baseline (a) and follow-up (b) axial FLAIR images reveal enlargement of the lateral ventricles with a rind of increased signal intensity along the margins of the ventricles (b), consistent with development of uncompensated hydrocephalus. There is also effacement of the cerebral sulci secondary to increased intracranial pressure.

Cerebritis

Cerebritis refers to focal infection of the brain parenchyma due to spread of infectious and inflammatory cells hematogenously or directly through perivascular spaces. With direct spread, the infection is often focal, while hematogenous spread often results in multifocal regions of parenchymal involvement. Patients typically present with seizures and/or focal neurological deficits, in addition to headaches.

On CT, cerebritis presents as a focal region of ill-defined hypoattenuation. Enhancement may be seen but is often ill-defined or thin and linear. MRI shows similar findings with ill-defined regions of increased T2 and decreased T1 signal intensity. Enhancement, when present, is similar to the pattern visualized on CT.[4] Regions of restricted diffusion may be seen[5] and may mimic an infarct acutely; the presence of overlying meningeal enhancement, if present, is a useful discriminator for infection. (Fig 5)

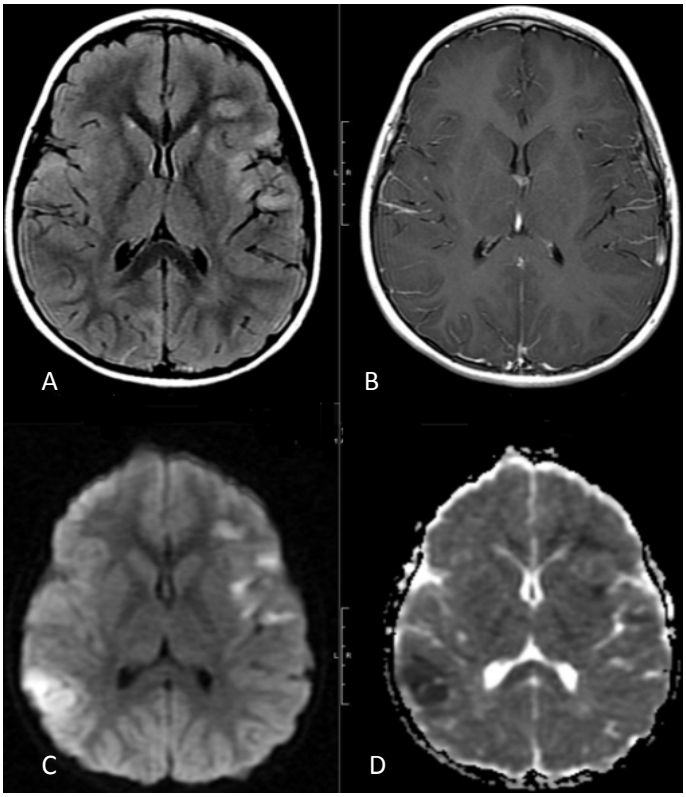

Figure 5. Cerebritis. Multiple axial images demonstrate multifocal regions of bilateral increased FLAIR signal intensity (a) involving the cortex and subcortical white matter with associated restricted diffusion, as evident by increased signal on DWI (c) and decreased signal on ADC maps (d). Axial T1 post contrast image (b) shows overlying leptomeningeal enhancement in the regions of cerebritis.

The treatment of cerebritis includes supportive care and intravenous antibiotics. If left untreated or if resistant to appropriate therapy, cerebritis may progress to a focal brain abscess. The imaging findings of the stages of evolution from cerebritis to abscess are detailed in the following section.

Brain abscess

Brain abscesses may result from hematogenous spread of a systemic infection, direct spread from an adjacent infection, progression of a focal region of cerebritis, or as the result of direct inoculation from trauma or surgery. Depending upon the etiology, abscesses may be solitary or multiple. The vast majority of abscesses are pyogenic with the remaining being atypical infections, which are more common in immunosuppressed patients.

There are four stages of abscess formation:[6] early cerebritis (1-3 days), late cerebritis (4-9 days), early capsule formation (10-13 days), and late capsule formation (14 days and beyond). As discussed in the previous section, early cerebritis presents as an ill-defined region of hypoattenuation on CT or increased T2 and decreased T1 signal intensity on MRI. There may be patchy enhancement without clear margins. Restricted diffusion may be seen. In the late cerebritis phase, the region of attenuation or signal abnormality becomes more focal with thin linear rim enhancement, which does not imply capsule formation at this stage. As the infectious process progresses through the early and late fibrous capsule formation stages (10 days and beyond), there is increased thick rim enhancement with surrounding vasogenic edema. The enhancing fibrous capsule is low in T2 signal intensity and is thinner towards the ventricles. Prominent central restricted diffusion is characteristic of a pyogenic infection. The surrounding vasogenic edema is more pronounced in the late capsule phase. Fig. 6 illustrates the imaging progression from cerebritis to abscess formation. In the cerebritis phases, intravenous antibiotics may be sufficient for treatment. Once the fibrous capsule forms, surgical drainage is often required.

Epidural abscess

Epidural abscesses are most often due to direct spread from paranasal sinus or mastoid infections. They may also occur as a result of adjacent calvarial processes, such as osteomyelitis or postsurgical complications.[7] As with other epidural collections, epidural abscesses are lenticular in shape, confined by sutures, and may cross midline.

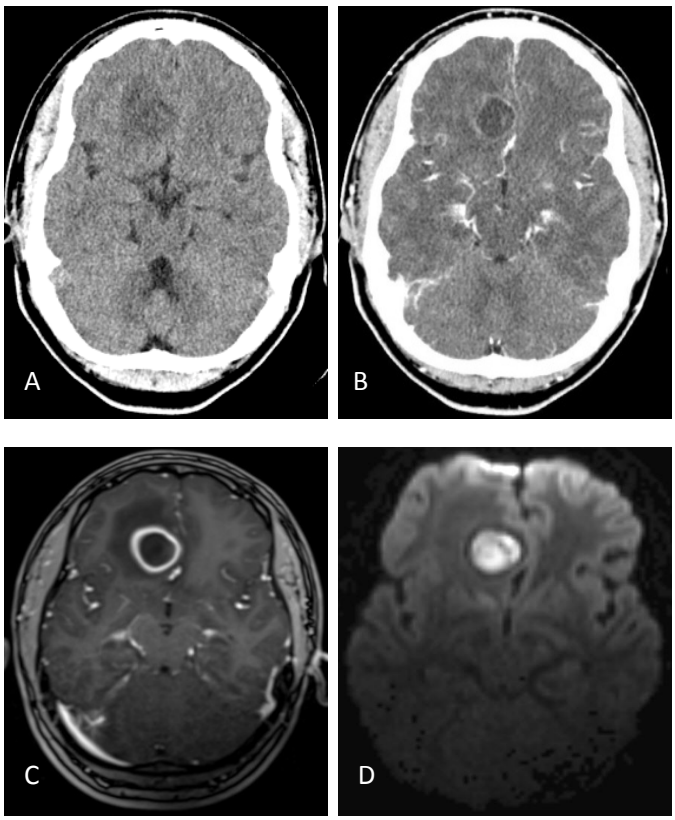

Figure 6. Cerebritis to abscess. Axial unenhanced CT image (a) reveals an ill-defined hypodensity within the right frontal lobe, consistent with early cerebritis. Several days later, axial enhanced CT image (b) shows a more focal hypodensity with thin, linear peripheral enhancement, consistent with late cerebritis. Axial T1 post contrast image with fat suppression (c) obtained the following week demonstrates thick rim enhancement with surrounding vasogenic edema, consistent with abscess. There is associated restricted diffusion centrally (d) (ADC map not shown).

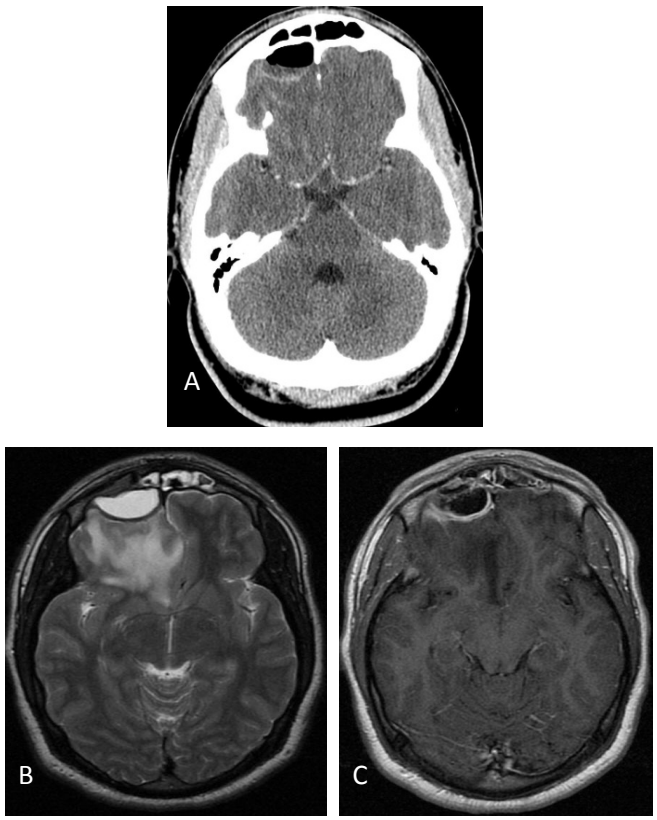

Figure 7. Epidural abscess. Axial enhanced CT image (a) reveals a focal rim enhancing epidural fluid collection with air-fluid level overlying the right frontal lobe. Axial T2 (b) and T1 post contrast (c) MR images show that the epidural collection is hyperintense on T2 and hypointense on T1 sequences. There is rim enhancement of the collection, as well as enhancement of the underlying dura. Prominent vasogenic edema with associated mass effect is noted within the underlying brain parenchyma. MR images show frontal sinus disease (b and c).

On CT, epidural abscesses are hypodense on CT and may have air-fluid levels. The abscess cavity demonstrates rim enhancement; enhancement of the underlying dura may also be seen (Fig 7a). Similar findings are noted on MRI where the epidural collections are hypointense on T1 and hyperintense on T2 sequences with similar enhancement patterns compared to CT (Fig. 7b and c).[8] The presence of restricted diffusion is variable but typically seen.

Treatment of epidural abscesses includes a combination of antibiotic therapy and surgical drainage. If left untreated, epidural abscesses may result in venous sinus thrombosis or extend through the dura to involve the subdural space, leptomeninges, or brain parenchyma.

Subdural empyema/effusion

Subdural empyemas most often result as a complication of meningitis or from direct spread of sinonasal or mastoid infections. As with other subdural processes, subdural empyemas are crescent-shaped, may cross sutures and extend along the interhemispheric fissure, but do not cross midline.

On CT, subdural empyemas are hypodense and typically have enhancement of the adjacent meninges.[9] Similar findings are noted on MRI with decreased T1 and increased T2 signal intensity, along with associated meningeal enhancement (Fig. 8).[8] As a general rule, subdural empyemas demonstrate restricted diffusion, while sterile subdural effusions do not. Effusions are commonly seen with *Haemophilus influenza* meningitis.

Treatment of subdural empyemas includes surgical drainage with antibiotic therapy. Complications include hydrocephalus, venous sinus thrombosis, and extension into the adjacent meninges and brain parenchyma.

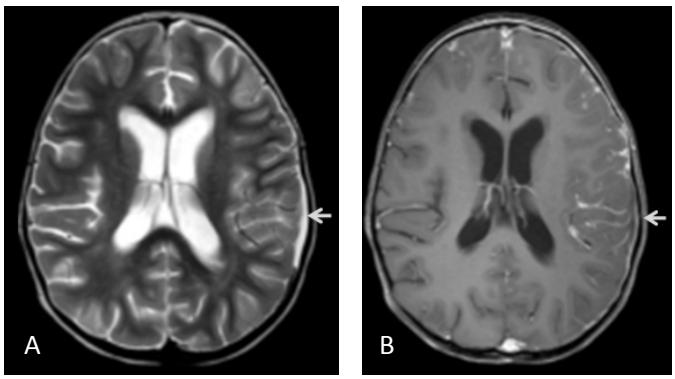

Figure 8. Subdural empyema. Axial T2 (a) and T1 post contrast with fat suppression (b) MR images demonstrate a mildly complex crescent-shaped T2 hyperintense and T1 hypointense subdural collection overlying the left temporal operculum and parietal lobes (arrows). There is a small amount of layering debris with decreased T2 signal (a). Post contrast image reveals mild leptomeningeal and overlying dural enhancement (b).

Viral encephalitis

There are numerous causes of viral encephalitis. The most common organisms which affect immunocompetent hosts include herpes simplex virus (HSV)-1 and those associated with mosquito-borne illnesses, such as West Nile, Eastern equine, and Japanese viral encephalitis.

HSV-1 is the most common cause of viral encephalitis, accounting for over 90% of cases. The viral infection may be primary or due to reactivation of a latent orofacial virus within the trigeminal ganglion, which is more common. HSV-1 encephalitis may occur in both immunocompetent and immunosuppressed individuals, although the morbidity and mortality is much higher in those who are immunosuppressed. Patients present acutely with fever, headache, seizures, mental status changes, and focal neurological deficits. If not recognized and treated promptly, the mortality rate approaches 70%.[10] Even with treatment, there is significant morbidity and mortality amongst affected patients; over half of patients whom survive have permanent neurological sequelae.

Imaging findings correspond to the site of reactivation within the limbic system. CT and MRI reveal regions of cortical and subcortical edema involving the temporal lobes, inferior frontal lobes, insula, and cingulate gyrus (Fig. 9). Most cases demonstrate bilateral but asymmetric involvement. The pattern of edema is in a nonvascular distribution, which is helpful in discriminating from an acute arterial infarct, and typically spares the deep gray matter. Foci of hemorrhage are commonly seen on CT. Patchy enhancement and regions of restricted diffusion are typically seen. Patients are treated with antiviral medications and supportive therapy. Complications include progression of the infection, venous sinus thrombosis, and intraparenchymal hemorrhage.

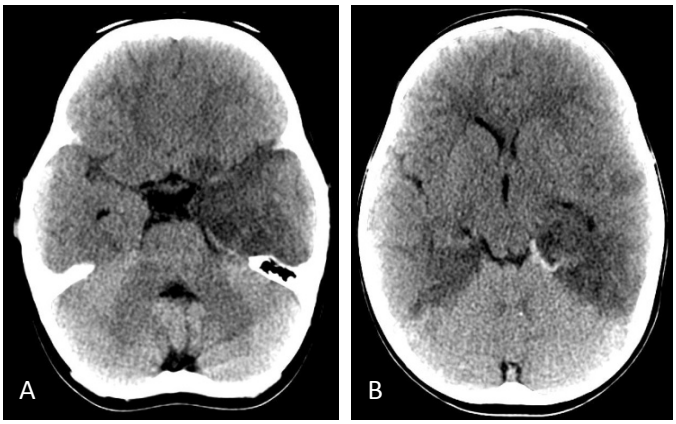

Figure 9. HSV-1 encephalitis. Axial unenhanced CT images demonstrate abnormal hypoattenuation and edema involving the cortex and underlying white matter of the left temporal (a and b) and inferior frontal lobes (a) in a nonvascular distribution. There is sparing of the basal ganglia (b). A curvilinear region of hemorrhage is noted along the posteromedial left temporal lobe (b).

Non-HSV viral encephalitides include West Nile, Eastern equine, and Japanese encephalitis, which are mosquito-borne illnesses prone to endemic regions. Patients present acutely with influenza-like symptoms, which then progress to meningitis or encephalitis with significant motor deficits. Flaccid paralysis and death occur in severe cases.

CT and MRI may be normal early in the disease process. As the disease progresses, focal regions of parenchymal signal abnormality are commonly seen. Parenchymal abnormalities include symmetric bilateral regions of hypodensity (CT) and signal abnormality (MRI) involving the thalami, lentiform nuclei, caudate, mesial temporal lobes,

and brainstem (Fig. 10).[11-14] Patchy enhancement and foci of hemorrhage may be seen. Overlying meningeal enhancement is relatively uncommon but is occasionally seen. Treatment consists predominantly of supportive care, as there currently are no effective antiviral therapies.

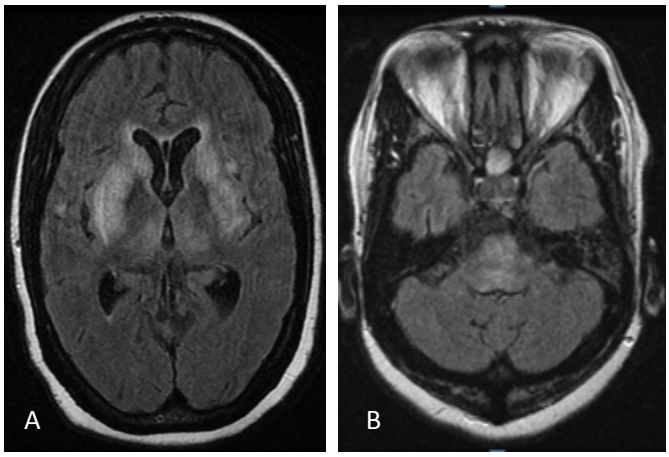

Figure 10. West Nile virus. Axial FLAIR images through the level of the deep gray matter structures (a) and brainstem (b) reveal symmetric abnormal regions of increased signal intensity involving the bilateral thalami, lentiform nuclei, caudate, and brainstem.

Rasmussen encephalitis

Rasmussen encephalitis is a rare progressive inflammatory neurological disorder of unknown origin. A viral or post-viral autoimmune etiology has been postulated, although the pathophysiology remains unclear. Patients present in childhood with persistent, relentless focal motor seizures (epilepsia partialis continua). As the disease progresses, patients experience hemiplegia and varying degrees of cognitive deficits. The disease process affects one cerebral hemisphere and results in progressive inflammation and atrophy.

Early on, MRI demonstrates abnormal edema and increased T2 signal intensity within the involved cerebral hemisphere. Chronically, findings are more characteristic with abnormal signal, asymmetric atrophy, and decreased perfusion and metabolism on the affected side (Fig. 11).[15,16] Treatment consists of functional hemispherectomy to prevent spread of the inflammatory process to the contralateral side.

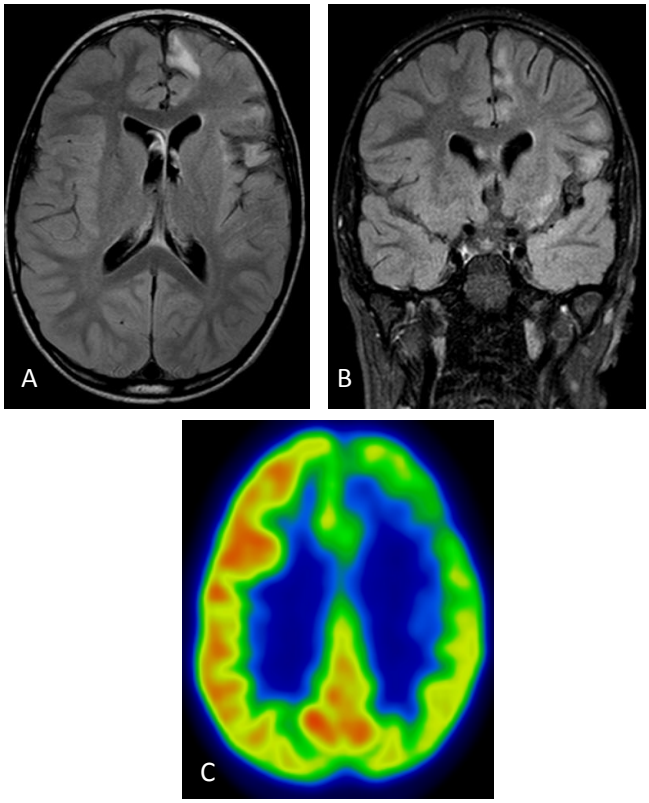

Figure 11. Rasmussen encephalitis. Axial (a) and coronal (b) FLAIR images reveal multifocal regions of increased signal intensity involving the cortex and subcortical white matter of the left frontal and temporal lobes. There is associated atrophy, which is most pronounced in the peri-Sylvian region. Axial image from an 18-FDG PET scan (c) reveals asymmetric decreased metabolism throughout the left cerebral hemisphere.

Neurocysticercosis

Neurocysticercosis is a parasitic infection that results from ingestion of undercooked pork or contaminated fruits and vegetables. It is the most common acquired cause of epilepsy worldwide. The causative organism is *Taenia solium*, a pork tapeworm. The disease is most prevalent in Central and South America where it is endemic. Those that frequently travel to these regions are susceptible to contracting the disease.

The ingested ova develop into larvae which become lodged within the musculoskeletal and central nervous systems. Within the CNS, lesions most often occur at the gray-white junction, followed by the ventricular system and subarachnoid spaces (racemose form). Patients often present acutely with seizures and headaches.

Imaging findings are dependent upon the stage of the disease: vesicular, colloidal, granular, and nodular.[17] During the vesicular stage, the lesions appear as nonenhancing cysts with a mural nodule, which is referred to as a scolex. In the colloidal stage, the cyst dies and there is an associated host inflammatory response. On imaging, there is a ring-enhancing lesion with surrounding vasogenic edema. During the granular stage, there is increased ring enhancement and surrounding vasogenic edema compared to the colloidal stage. In the final nodular stage, the lesions are calcified without adjacent edema or enhancement. (Fig. 12)

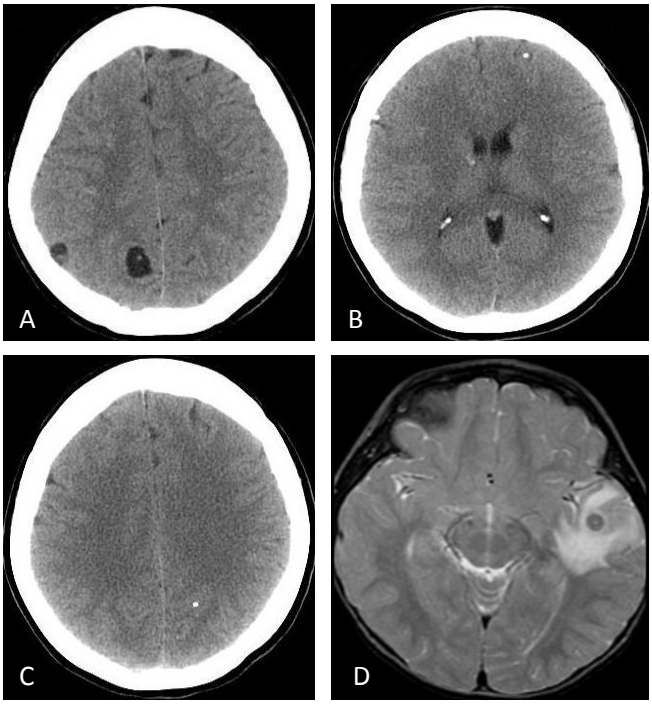

Figure 12. Neurocysticercosis. Axial CT images (a thru c) demonstrate parenchymal lesions in the vesicular stage with a cyst and scolex (a) and the nodular stage with multiple calcified lesions (b and c). Axial T2 image in a different patient (d) shows the granular stage with a small lesion within the left temporal lobe with moderate vasogenic edema. (*Images a thru c courtesy of Anand Rao, M.D.; image d courtesy of Paul Sherman, M.D.*)

Summary

In summary, there are various etiologies of CNS infections which affect the immunocompetent host. Clinical presentations vary based upon the age of the patient and nature of the infection. Knowledge of the characteristic imaging patterns and potential complications of various infectious processes will allow for prompt diagnose and treatment, thus minimizing morbidity and mortality associated with these entities.

The views expressed in this material are those of the author, and do not reflect the official policy or position of the U.S. Government, the Department of Defense, or the Department of the Air Force.

References

1. Chang KH, Han MH, Roh JK, et al. Gd-DTPA-enhanced MR imaging of the brain in patients with meningitis: comparison with CT. Am J Neuroradiol 11: 69-76, 1990
2. Stuckey SL, Goh TD, Heffernan T, et al. Hyperintensity in the subarachnoid space on FLAIR MRI. Am J Roentgenol 189: 913-21, 2007
3. Hughes DC, Raghavan A, Mordekar SR, et al. Role of imaging in the diagnosis of acute bacterial meningitis and its complications. Postgrad Med J 86: 478-85, 2010
4. Falcone S, Post M. Encephalitis, cerebritis, and brain abscess: pathophysiology and imaging findings. Neuroimaging Clin N Am 10: 333-53, 2000
5. Tung GA, Rogg JM. Diffusion-weighted imaging of cerebritis. Am J Neuroradiol 24: 1110-13, 2003
6. Hygino da Cruz LC, Domingues RC. Intracranial infections. In: Atlas SW. Magnetic resonance imaging of the brain and spine, 4th ed. Philadelphia, PA: Lippincott Williams & Wilkins, 2008
7. Sharif HS, Ibrahim A. Intracranial epidural abscess. Br J Radiol 55: 81-84, 1982
8. Weingarten K, Zimmerman RD, Becker RD, et al. Subdural and epidural empyemas: MR imaging. Am J Roentgenol 152: 615-21, 1989
9. Weisberg L. Subdural empyemas: clinical and computed tomographic correlations. Arch Neurol 43: 497-500, 1986.
10. Ahmad N, Ray CG, Drew WL. Herpesvirus. In: Ryan KJ, Ray CG, Ahmad N, et al. Sherris Medical microbiology, 5th ed. New York, NY: McGraw-Hill, 2010
11. Petropoulou KA, Gordon SM, Prayson RA, et al. West Nile virus meningoencephalitis: MR imaging findings. Am J Neuroradiol 26: 1986-95, 2005
12. Abe T, Kojima K, Shoji H, et al. Japanese encephalitis. J Magn Reson Imaging 8: 755-61, 1998
13. Kumar S, Misra UK, Kalita J, et al. MRI in Japanese encephalitis. Neuroradiology 39: 180-4, 1997
14. Siu JCW, Chan CY, Wong YC, et al. Magnetic resonance imaging findings of Japanese encephalitis. J HK Coll Radiol 7: 76-80, 2004
15. Geller E, Faerber EN, Legido A, et al. Rasmussen encephalitis: complementary role of multitechnique neuroimaging. Am J Neuroradiol 19: 445-9, 1998
16. Fiorella DJ, Provenzale JM, Coleman RE, et al. 18F-Fluorodeoxyglucose positron emission tomography and MR imaging findings in Rasmussen encephalitis. Am J Neuroradiol 22: 1291-99, 2001
17. Kimura-Hayama ET, Higuera JA, Corona-Cedillo R, et al. Neurocysticercosis: radiologic-pathologic correlation. RadioGraphics 30: 1705-19, 2010

Vascular Malformations of the Brain: Radiologic and Pathologic Correlation

Alice Boyd Smith, Lt. Col. USAF MC

Division of Neuroradiology, Uniformed Services University of the Health Sciences, Bethesda, MD

Vascular malformations involving the brain are divided into subgroups, including arteriovenous malformations (AVM), developmental venous anomalies (DVA), cavernous malformations and capillary telangiectasias. These lesions are further categorized into those that demonstrate shunting from arterial to venous systems (i.e. the AVM), and those that do not have shunting (DVA, cavernous malformation, and capillary telangiectasia). In addition, mixed malformations (i.e. lesions composed of more than one malformation) occasionally occur. The most common lesions seen within a mixed malformation are the DVA in combination with a capillary telangiectasia. Understanding the associated imaging findings and potential complications of these lesions assists in determining the appropriate treatment options.

Arteriovenous Malformation

Arteriovenous malformations are high flow shunts between the arterial and venous systems without an intervening capillary bed. These lesions are subdivided into the classic arteriovenous malformation and the arteriovenous fistulas.

Classic Arteriovenous Malformation

The classic AVM (also known as pial AVM) results from an abnormal connection between the arteries that normally supply the brain parenchyma and the veins that would normally drain this region. Imaging and pathology reveal an enlarged feeding artery, a nidus consisting of numerous arteriovenous shunts and dysplastic vessels, and an enlarged draining vein. The nidus can be characterized as glomerular (compact and the intervening brain is not normal), or diffuse (normal brain is interspersed between the abnormal vessels). (Fig. 1) The glomerular form is the most commonly encountered, whereas the diffuse form is rare, but is the type found in cerebrofacial arteriovenous metameric syndrome (CAMS).[1] CAMS is a rare, non-hereditary disorder consisting of brain-retino-facial angiomatosis resulting multiple AVMs involving the face, eye and brain. (Fig. 2) AVMs occur anywhere in the brain or spinal cord, but the majority are supratentorial. Ninety-eight percent of these lesions are solitary. If multiple AVMs are seen, syndromes such as hereditary hemorrhagic telangiectasia (HHT) or CAMS need to be considered.[2]

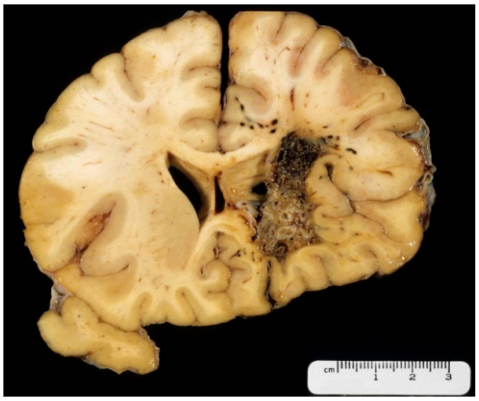

Figure 1: AVM with glomerular nidus. Photograph of a gross specimen reveals a compact nidus adjacent to the left lateral ventricle with no intervening normal brain. Notice that the left hemisphere is smaller than the right. This finding results from chronic ischemia due to vascular steal.

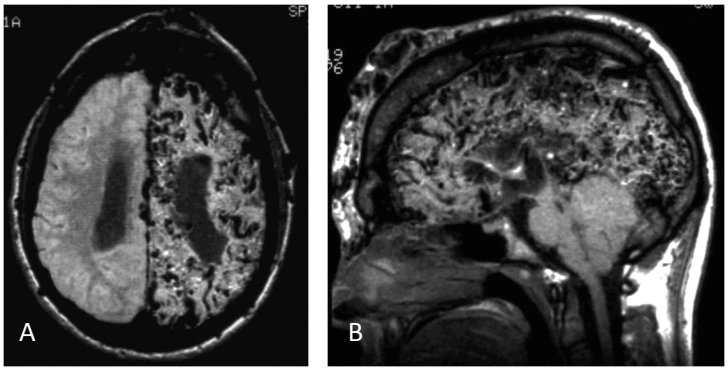

Figure 2: CAMS. Axial FLAIR (A) and sagittal T1 (B) reveal multiple flow voids consistent with an extensive, diffuse AVM involving the left hemisphere, as well as the soft tissues of the face and scalp.

The peak age for presentation is in the 20 to 40 year old age group (mean age approximately 30 years).[3] Fifty percent of these patients present with hemorrhage, and the risk for hemorrhage is 2-4% per year.[4,5] Once a hemorrhage occurs, there is a 6-18% risk of rehemorrhage within the first year.[4] This rate gradually returns to 2-4% per year. The mortality rate with the first hemorrhage is approximately 10%. Each successive hemorrhage has an increasing mortality rate, and by the time the patient has their 3rd hemorrhage the mortality rate reaches 20%.[6] Twenty-four to 30% of patients present with seizure unrelated to hemorrhage.[3,7] Other non-hemorrhage presentations include headache and focal neurologic deficit.

The underlying etiology of AVMs remains unknown, but various hypotheses suggest they are congenital in origin and result from either retention of early embryonic vascular connections, alteration of these vascular connections, or alterations of the embryonic vascular remodeling process in combination with angiogenesis or dysgenesis of the capillary system.[8,9] More recent hypotheses challenge the congenital origin and suggest that these lesions may result from angiogenic and inflammatory responses to a postnatal event, and several case reports describe de novo development of AVMs.[10,11] AVMs demonstrate a dysregulated angiogenesis and undergo continued vascular remodeling. Vascular endothelial growth factor (VEGF), which mediates endothelial proliferation, has been found to be elevated in these patients.[12]

In the glomerular form, neural tissue is typically found between the dysplastic vessels of the nidus. (Fig. 3) This tissue is frequently atrophic and gliotic and calcification may be seen. The surrounding brain may develop gliosis resulting from vascular steal related to the AVM.

Imaging findings of AVMs vary depending on the size of the lesion, and presence of hemorrhage or calcification. On CT calcification may be seen in up to 30% of cases.[13] CT and MR angiography can be utilized to demonstrate the feeding arteries and draining veins. Smaller lesions may be difficult to visualize on non-contrast CT since they are filled with flowing blood that is isoattenuating to slightly hyperattenuating to normal brain. On MRI, flow voids are seen within the lesion, giving the classic "bag of worms" appearance. T2* GRE may reveal hypointense blooming if hemorrhage or calcification is present. In some cases, T2 hyperintensity is identified in the adjacent brain parenchyma consistent with areas of gliosis. (Fig. 4) Conventional angiography is still considered the "gold standard" for demonstrating the internal angioarchitecture. The internal carotid, external carotid and vertebral circulation must all be evaluated, since approximately 27% of AVMs have a dual arterial supply.[14] Conventional angiography is considered to be the best method to detect intranidal aneurysms.

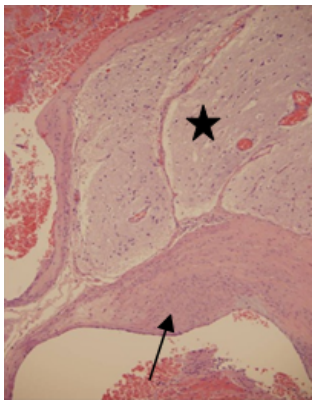

Figure 3: AVM. Photomicrograph of a hematoxylin-eosin (H-E) stain of a glomerular type AVM. The vessel walls are dysplastic with varying degree of thickness (arrow). There is intervening brain tissue (star), which is gliotic.

There are characteristics of AVMs that may be associated with a greater risk of hemorrhage. One of the greatest risk factors for hemorrhage is evidence of prior hemorrhage.[15] Utilization of gradient echo imaging can assist in detecting evidence of prior hemorrhage. The location of the lesion plays a role. AVMs in periventricular regions, in the basal ganglia, or involving the thalamus are at greater risk. These regions are supplied by small perforating arteries that are not designed to handle

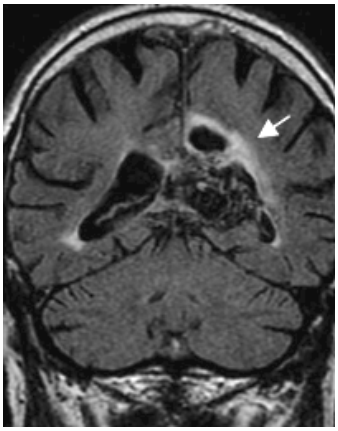

Figure 4. AVM with adjacent gliosis. Coronal T2 FLAIR reveals flow voids associated with a periventricular AVM on the left. There is adjacent increased T2 signal consistent with gliosis (arrow).

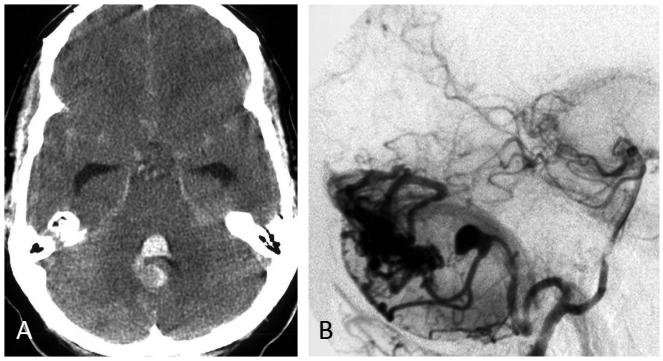

Figure 5. AVM with hemorrhage and pedicle aneurysm. (A) Non-contrast CT reveals intraventricular hemorrhage within the 4th ventricle. There is associated hydrocephalus. (B) Lateral digital subtraction angiography (DSA) from a right vertebral artery injection reveals an aneurysm along the posterior inferior cerebellar artery which is supplying the right cerebellar AVM. Note the "beaked" appearance of the aneurysm suggesting that it has ruptured and is the source of hemorrhage.

the increased flow resulting from the AVM. Posterior fossa lesions also have a higher risk of hemorrhage. Assessment for pedicle aneurysms (i.e. those on the feeding artery) or intranidal aneurysms is important, as these may be a source of hemorrhage. (Fig. 5) Another important risk factor is obstruction of venous outflow, which results in increased pressure. The central draining veins are more prone to developing stenosis. Single venous drainage is also associated with higher risk.[1]

Other risks from AVMs include nonhemorrhagic neurologic deficits. Imaging findings suggesting a higher risk of neurologic deficit include evidence of arterial steal, high flow shunt, mass effect or hydrocephalus, venous congestion or outflow obstruction, and long pial course of the draining vein.[1]

AVMS can be treated with surgery, endovascular embolization, radiosurgery, or a combination of these methods. Certain characteristics of the AVM help predict the risk of surgical morbidity and mortality. The Spetzler Martin grading scale is a method of scoring AVMs to predict surgical morbidity and mortality. The size, location, and venous drainage of the lesion is assessed and graded on a point scale (Table 1). If the score is a one or two, the risk of surgical mortality is less than 1% and the surgical morbidity is less than 10%.[16]

Size	Small (<3cm) = 1
	Medium (3-6 cm) = 2
	Large (>6 cm) = 3
Location	Noneloquent = 0
	Eloquent = 1
Venous drainage	Superficial = 0
	Deep = 1

Table 1. Spetzler Martin Grading Scale for AVMs

Arteriovenous Fistulas

Arteriovenous fistulas are distinguished from AVMs by the presence of a direct, high flow fistula between artery and vein. There is no intervening nidus. These include the dural arteriovenous fistula (dAVF), the cavernous carotid fistula (CCF) and the vein of Galen malformation (VOG).

Dural Arteriovenous Malformation

The dural arteriovenous malformation (dAVF) consists of arteriovenous shunts within the dura. Arterial supply is from meningeal branches and drainage is via either dural sinuses or meningeal or subarachnoid veins. They comprise 10-15% of intracranial vascular malformations.[17]

There are 2 types of dAVF – adult and infantile.[18] The infantile form is a rare congenital condition in which multiple high-flow arteriovenous shunts occur involving several thrombosed dural sinuses. Fetal US reveals a hypoechoic heterogeneous lesion centered on the torcula. Fetal MR confirms the dural location of the mass. T1-weighted images reveal heterogeneous signal with areas of hyperintensity; hypointensity is typically seen on the T2-weighted images. (Fig. 6) In one study in which pathologic evaluation was performed, a large dural hematoma was noted in the posterior fossa, corresponding to thrombus in the enlarged cerebral veins.[18] The etiology of the infantile from is postulated to be a response to venous obstruction in the fetus.[19]

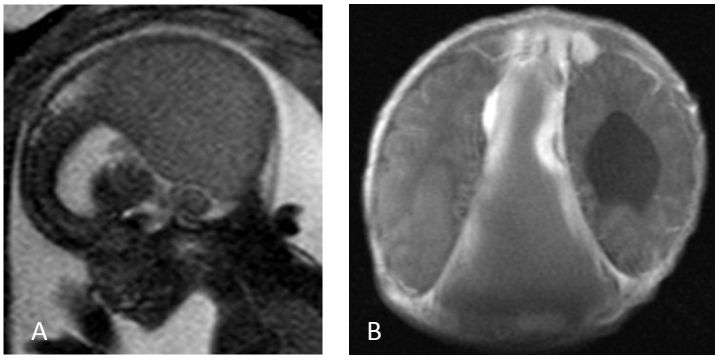

Figure 6. Fetal dural sinus arteriovenous fistula. (A)SSFSE T2 weighted image of a 22 week fetus demonstrates a large, hypointense mass in the dural space centered on the torcula. (B) Coronal T1 post contrast performed on day of life 1 demonstrates an enlarged sagittal sinus with thrombosis.

The adult form typically presents in middle-aged to older patients and is thought to be secondary to dural sinus thrombosis resulting from trauma or inflammation, but the etiology is not completely understood.[20] One of the proposed etiologies involves 3 steps: 1) initial thrombosis of a dural sinus leading to impaired venous drainage and increased sinus pressure; 2) secondary dilatation of physiologic shunts between the thrombosed sinus and arterial structures (typically extracranial); 3) recanalization of the thrombosed sinus allowing for direct arterial shunting into the sinus.[21] These lesions consist of tiny vessels in the wall of a thrombosed dural venous sinus. The most common locations involve the transverse-sigmoid sinuses and cavernous sinus.[21] The clinical features vary from mild complaints, such as headache, vertigo, and tinnitus to neurologic deficits and hemorrhage. In general, symptoms are related to the drainage pattern and location.[21]

Different classification systems exist for the dAVF, one of which is the Cognard classification. (Table 2) The more cortical drainage present, the greater the risk of hemorrhage. Davies, et al. categorized them as benign or aggressive lesions depending on the presence or absence of retrograde leptomeningeal venous drainage (RLVD).[22] In type IV dAVF by the Cognard classification, there is direct cortical drainage and venous ectasia; two-thirds of these cases will have hemorrhage.[23] The presence of RLVD on angiography indicates a clinically aggressive lesion and is an indication for active treatment, which may consist of endovascular embolization, surgical resection, or radiosurgery.

Type	Venous drainage
I	Antegrade sinus drainage
II	Insufficient sinus drainage
IIa	Retrograde sinus drainage
IIb	Retrograde CVR
IIa+IIb	Retrograde sinus drainage and CVR
III	CVR only without venous ectasia
IV	CVR only with venous ectasia
V	Spinal venous drainage

CVR = cortical venous reflux

Cognard et al. Cerebral dural arteriovenous fistulas: clinical and angiographic correlation with a revised classification. Radiology 1995;194:671-680.

Table 2. Cognard Classification of dAVF

Non-contrast CT may be normal. CT angiogram potentially reveals tortuous dural feeders and an enlarged dural sinus. In aggressive cases, enlarged cortical draining veins can be seen. (Fig. 7) On MRI, flow voids may be seen around the involved dural sinus, and the sinus may be thrombosed. T2

hyperintensity may be seen in the adjacent brain due to vascular steal. (Fig. 8) White matter edema suggests venous congestive encephalopathy. The MRA may be negative, but an occluded sinus with collateral flow may be seen on MRV. Conventional angiography reveals multiple arterial feeders, most commonly from dural or transosseous branches of the external carotid artery, but tentorial or dural branches from the internal carotid or vertebral arteries can also be involved. The involved dural sinus is often thrombosed. Flow reversal may be seen in the dural sinus and the cortical veins. In clinically aggressive cases, tortuous engorged pial veins are seen. This is referred to as the pseudophlebitic pattern. (Fig. 9)

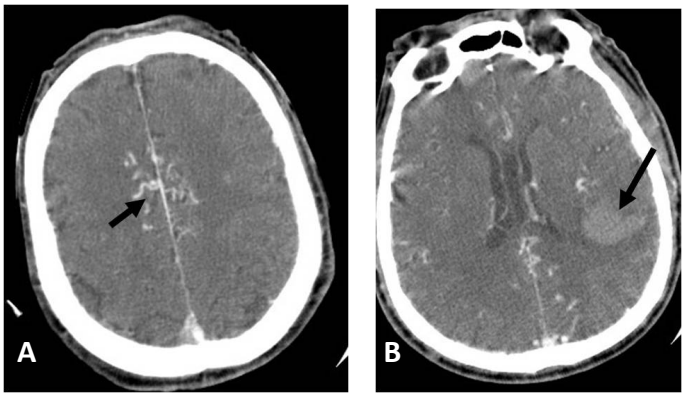

Figure 7. Clinically aggressive dAVF. (A) CT angiogram reveals multiple cortically draining veins (arrow). (B) Hemorrhage is present in the left temporoparietal region (arrow).

Figure 8. dAVF. Axial T2-weighte image reveals flow voids adjacent to the region of the transverse sinus. The torcula is dilated. T2 hyperintensity and volume loss are seen in the region of the dAVF corresponding to gliosis secondary to vascular steal.

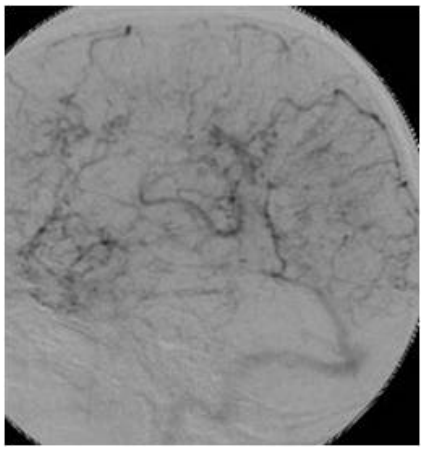

Figure 9. Clinically aggressive dAVF. Lateral DSA in the late venous phase from injection of the common carotid artery demonstrates numerous engorged pial veins – the "pseudophlebitic" pattern.

Carotid Cavernous Fistula

The carotid cavernous fistula (CCF) consists of an abnormal communication between the internal carotid artery (ICA) and cavernous sinus resulting in enlargement of the cavernous sinus. The superior ophthalmic vein (SOV) will typically be enlarged; however, in some cases the dilated SOV will be contralateral to the CCF. The Barrow system classifies CCF by arterial supply and venous drainage. (Table 3) These are either direct and high flow due to a direct communication between the ICA and the cavernous sinus, or indirect and lower flow due to a connection between the cavernous sinus and dural ICA or external carotid artery (ECA) branches. A direct CCF is usually due to trauma or intracavernous rupture of an ICA aneurysm. The indirect form typically occurs spontaneously and is only rarely secondary to trauma.[24] Patients typically present with ocular symptoms – pulsating exophthalmos, orbital bruit, chemosis – resulting from anterior venous drainage. More aggressive symptoms such as intracranial hemorrhage are rare.[25]

Imaging findings reveal orbital proptosis, enlarged extraocular muscles, dilated superior ophthalmic vein, and enlargement of the cavernous

sinus on the involved side. Normally, the walls of the cavernous sinus should always be straight or concave. MRI imaging reveals an increase in the number of flow voids within the involved sinus. (Fig. 10) Angiography reveals prompt filling of the superior ophthalmic vein in the arterial phase. (Fig. 11) Conventional angiography may help elucidate the etiology and be utilized for embolization with coils or glue.

Type	Arterial supply and venous drainage
A	Direct ICA-cavernous sinus high-flow shunt
B	Dural ICA branches-cavernous shunt
C	Dural ECA branches-cavernous shunt
D	ECA/ICA dural branches shunt to cavernous sinus

ICA = internal carotid artery, ECA= external carotid artery
Barrow DL et al. Classification and treatment of spontaneous carotid-cavernous sinus fistulas. J Neurosurg 1985;62:248-56.

Table 3. Barrow's Classification of Carotid Cavernous Fistulas

Figure 10. Carotid cavernous fistula. Axial T2-weighted image reveals multiple flow voids within the left cavernous sinus (arrows). The wall of the cavernous sinus is convex on the left. Left orbital proptosis is present and the extraocular muscles are enlarged and edematous. There is inflammation of the periorbital and intraconal fat.

Vein of Galen Malformation

The vein of Galen malformation (VOGM) is an arteriovenous fistula resulting in dilatation of the median prosencephalic vein (MPV), which is the embryonic precursor to the vein of Galen.[26] The exact etiology of the malformation is not known,

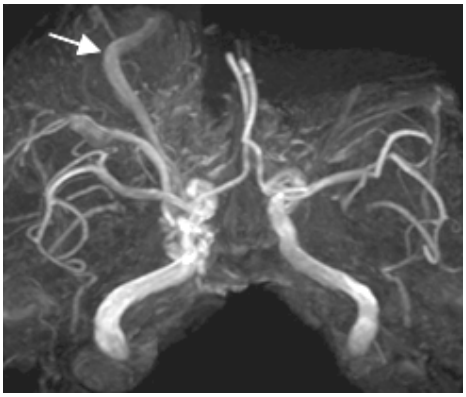

Figure 11. Carotid cavernous fistula. Maximum intensity projection from a 3D time of flight MRA demonstrates increased signal in the right cavernous sinus, and the right superior ophthalmic vein is visible (arrow).

but the arteriovenous shunts with the MPV are thought to occur during 6 to 11 weeks gestation.[26] The resultant increased flow through the MPV prevents the transient fetal venous drainage pattern from involuting. In 50% of these patients, the straight sinus does not form and the vein drains via a falcine sinus. (Fig. 12) These lesions most commonly present in the neonatal period and are the most common cause of non-cardiac congestive heart failure in the newborn period. Patients may develop ischemic damage involving the brain parenchyma due to a vascular steal.[27] Occasionally, they first present later in infancy and rarely, they can present in adulthood. Older infants usually present with milder cardiac symptoms, most often coming to medical attention due to hydrocephalus from compression of the aqueduct or posterior 3rd ventricle. Seizures may also occur.[26] Children and adults may present with headaches or subarachnoid hemorrhage. Patients presenting in the neonatal period typically have a worse prognosis than those presenting later. They are more common in males than in females with a ratio of 2:1.

VOGM are classified as either choroidal or mural. In the choroidal form, there are multiple feeders from the pericallosal, choroidal, and thalmoperforating arteries resulting in an extensive arterial network between the arterial feeders and

the dilated venous pouch. (Fig. 13) In the mural form, there are few feeders from collicular or posterior choroidal arteries that end directly within the wall of the MPV. Over 90% of these lesions are choroidal, and the choroidal form typically presents in neonates. The mural form usually presents in infancy.

Figure 12. Vein of Galen malformation. Sagittal T1-weighted image reveals abnormal flow voids communicating with an enlarged falcine sinus (arrow).

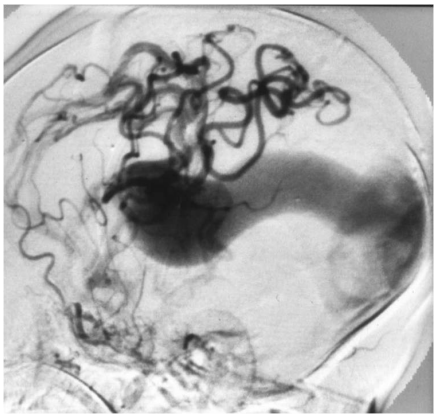

Figure 13. Choroidal vein of Galen malformation. DSA lateral view after internal carotid injection shows multiple feeds predominantly from pericallosal and choroidal arteries. Early filling of the enlarged venous pouch is demonstrated.

CT imaging reveals a dilated venous pouch. Mass effect from the dilated vein may result in hydrocephalus due to compression of the aqueduct of Sylvius. Parenchymal atrophy may be seen due to vascular steal, and calcifications may be seen secondary to ischemic brain damage. (Fig. 14) Rarely, intraventricular hemorrhage can occur. CT angiography can be utilized to map the arterial and venous structures.[28] However, catheter angiography is still the gold standard for the evaluation of VOGM angioarchitecture. On MR, T1 hyperintensity may be seen in the pouch if a thrombus is present. T1 hyperintensity can also be seen in the brain parenchyma in the setting of ischemia or calcification. Reduced diffusion may be seen in the setting of acute infarction. In severe cases, diffuse brain destruction, referred to as melting brain, may be seen.

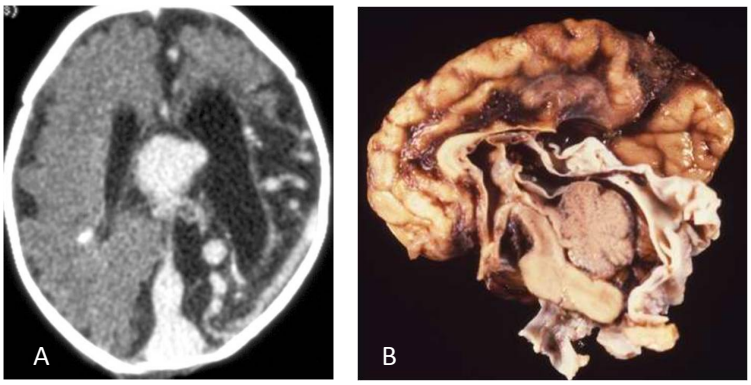

Figure 14. Vein of Galen malformation. (A) Axial post contrast CT demonstrates enhancement of the enlarged venous pouch. Encephalomalacia with ex vacuo dilatation of the left lateral ventricle is noted. (B) Photograph of gross specimen demonstrates marked cerebral atrophy due to the vascular steal along with the enlarged venous pouch.

The timing of endovascular treatment is determined by the patient's clinical presentation. If congestive heart failure is refractory to medical therapy in the newborn period, emergent embolization is necessary.[27] If the patient is not in heart failure, then embolization can be delayed until 5-6 months, reducing the risk of affecting brain maturation.[29] Embolization may be achieved through the arterial or venous route. The arterial method is preferred since occlusion of the venous aneurysm may interfere with deep venous drainage or result in perforation of the venous aneurysm.[30,31]

Prior to the development of endovascular embolization, the mortality rate for neonates with VOGM was 100%.[27] In a recent study by Lasjaunias, et al., the mortality rate for neonates was 52%.[32] The treatment of associated hydrocephalus is controversial. Shunt placement may alter venous drainage which can exacerbate brain damage, and is usually reserved for refractory hydrocephalus after transcatheter embolization performed.[27]

Cavernous malformation

Cavernous malformations (CM) are slow flow lesions, which in the past resulted in them being referred to as "occult" or "cryptic" malformations, since they did not show up on catheter angiography. They occur in about 0.4 – 0.8% of the population, and account for 10-15% of all CNS vascular lesions, making them the second most common CNS vascular malformation after DVAs.[33,34] These lesions may be inherited in an autosomal dominant pattern in up to 20% of cases, in which case there are multiple lesions in over 50% of cases.[34,35] The remainder are sporadic, and in these cases only 10-20% will have multiple lesions.[33,34] Patients most commonly present in the 3rd or 4th decades of life, but one-quarter of cases present in infancy or childhood.[36] Patients may present with seizure, focal neurologic deficits, or acute intracranial hemorrhage; however, most are asymptomatic at the time of diagnosis.[34] The location of the lesions plays a role in the symptomatology. Those that are infratentorial tend to more commonly present with hemorrhage, whereas supratentorial lesion are more likely to present with seizure.[37,38]

CMs are vascular hamartomas comprised of variable sized intercapillary vascular spaces, sinusoids, and larger cavernous spaces without intervening brain tissue. (Fig. 15) These lesions lack smooth muscle support and are filled with blood or thrombus. CM are associated with hemosiderin, whether or not they have overtly hemorrhaged, which may be related to absent or diminished tight junctions seen on ultrastructural studies. This implies a localized loss of the blood-brain barrier and diminished vascular stability.[35,39]

Figure 15. Cavernous malformation. Photograph of a gross specimen reveals a compact mass of thin walled vascular channels without any intervening brain.

CMs may occur in combination with DVAs, and there is evidence to suggest a causative link between the two. Dan Millan Ruiz, et al. reported the presence of hemosiderin laden macrophages in the region of the DVA.[40] Suggested etiologies for this finding include blood diapedesis through the walls of the venous radicals of the DVA or rupture of a venous radical.[41,42] It is hypothesized that repeated microhemorrhages activate angiogenic growth factors that over time result in the formation of a CM.[43]

On imaging, these lesions have little or no mass effect unless they are complicated by hemorrhage. The risk of hemorrhage is 0.25-0.6% per year.[38,44] It has been reported that CMs associated with DVAs tend to hemorrhage more frequently than isolated malformations.[45] Once hemorrhage occurs, the annual risk of recurrent hemorrhage goes up to 4.5%.[44] However, some have reported that the increased risk is only elevated for the first 2-3 years after the initial hemorrhage, and then drops back to baseline.[46]

CT imaging is frequently negative, especially if the lesion is less than 1 cm, or in the absence of

calcification or hemorrhage.[34] Calcification may be seen in up to 60%. On T2-weighted imaging, a peripheral hemosiderin rim may result in a black "halo" around the lesion. (Fig. 16) The adjacent brain parenchyma is normal, and surrounding vasogenic edema is not present unless the lesion is complicated by hemorrhage. (Fig. 17) These lesions may have internal areas of thrombosis or hemorrhage, and these blood products are of varying ages. The presence of methemoglobin results in hyperintensity on T1 images. Findings on post-contrast imaging are variable, with enhancement ranging from none to moderate. It is important to look for a DVA on post contrast imaging, as the location of the DVA will be important if surgical treatment is planned in order to avoid inadvertent damage to venous drainage.

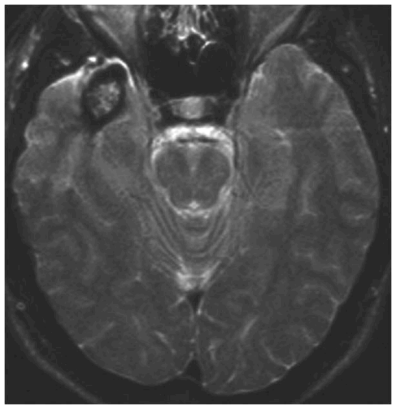

Figure 16. Cavernous malformation. Axial T2-weighted image reveals a cavernous malformation within the right temporal lobe. The low signal rim corresponds to hemosiderin deposition.

Treatment for these lesions includes observation in cases where the lesions are asymptomatic or surgical resection. In patients who present with seizures, surgical treatment should be utilized if their seizures increase in severity or do not respond to antiepileptic drugs. In patients with hemorrhage, a conservative approach is usually initially taken, but if the hemorrhage causes severe neurological symptoms or recurs, then surgery should be considered. Radiosurgery may be considered as an alternative for those lesions that are progressively symptomatic but surgically inaccessible.[34]

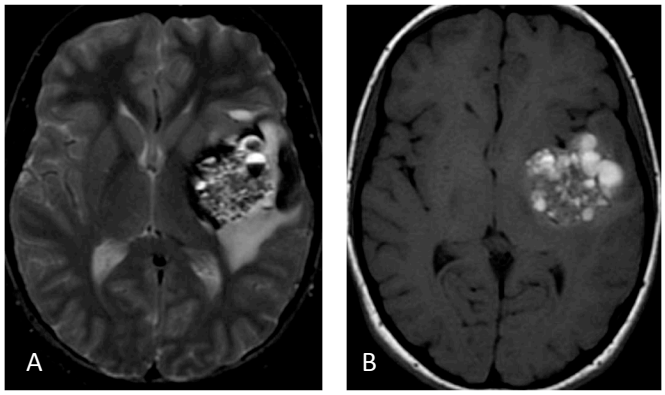

Figure 17. Hemorrhagic cavernous malformation. (A) Axial T2-weighted image reveals a cavernous malformation with mild mass effect and surrounding vasogenic edema secondary to hemorrhage. Fluid-fluid levels are seen within the lesion, and a partial hemosiderin rim is present along the medial aspect. (B) Axial T1-weighted image without contrast reveals a "popcorn ball" lesion with areas of hyperintensity within the CM corresponding to methemoglobin.

Developmental Venous Anomaly

Developmental venous anomalies (DVA) are the most commonly encountered cerebral vascular malformations. In a series of 4,069 brain autopsies, they were encountered in 2.6% of cases.[47] They are thought to represent anatomic variants that arise from maldevelopment of fetal cortical venous drainage, most likely resulting from recruitment of parenchymal veins to compensate for loss or absence of a portion of the cerebral venous system.[42] DVAs are comprised of enlarged medullary veins that drain into a venous trunk that flows into a dural sinus or deep ependymal vein, resulting in a "palm tree" or *caput medusa* appearance on imaging. (Fig. 18) These lesions are usually solitary, although two or more draining separate regions of the brain have been reported in 1.2-16% of cases.[42,48]

Patients are usually asymptomatic with the DVA representing an incidental finding on imaging, but acute thrombosis of the collecting vein may result in hemorrhage or infarction.[42] Associated cavernous malformations, which have been reported to be

associated with DVAs in 13-40% of cases, may also be an etiology of hemorrhage or seizure.[49,50]

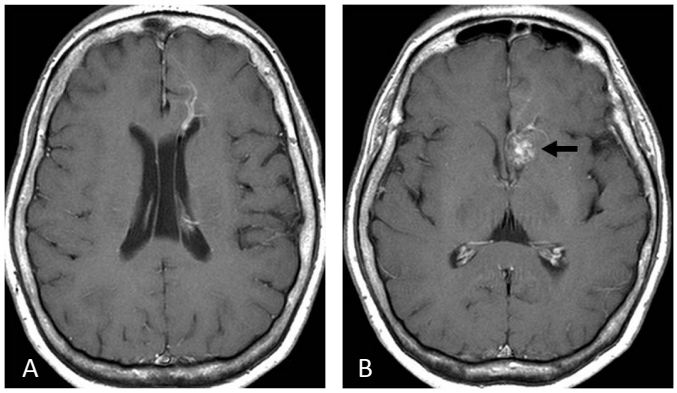

Figure 18. Developmental venous anomaly. (A) Axial T1 post contrast reveals a "palm tree" appearance of a left frontal developmental venous anomaly that drains into a deep ependymal vein. (B) Axial T1 post contrast demonstrates an associated cavernous malformation (arrow).

The classic imaging finding of the *caput medusa* allows for ease of diagnosis on both contrast enhanced CT or MRI. On non-contrast CT, the draining vein will typically appear isoattenuating to slightly hyperattenuating to the cortex, but if acutely thrombosed, then a markedly hyperattenuating vein may be seen. MR imaging may reveal flow voids in the region of the medullary veins and draining vein depending on size. Occasionally on MR imaging, T2 hyperintensity may be seen in the region of a DVA. This may occur in completely asymptomatic patients, but can also reflect acute edema from thrombosis, or gliosis from chronic outflow obstruction. In a study of 84 DVAs by San Millan Ruiz, et al. utilizing CT and MRI imaging, brain parenchymal abnormalities were noted in close to two-thirds of cases. These findings included locoregional brain atrophy in 29.7%, white matter lesions in 28.3%, cavernous malformations in 13.3%, and dystrophic calcifications in 9.6%. They also reported intraparenchymal hemorrhage possibly related to the DVA in 2.4% and stenosis involving the collecting vein in 13.1%.[50] Catheter angiography can be utilized to evaluate the hemodynamic behavior of developmental venous anomalies in patients presenting with hemorrhagic or ischemic complications in the drainage territory of a DVA.[42]

DVAs are "leave alone" lesions in that resection will result in venous infarction of the area drained by the DVA.

Capillary Telangiectasia

Capillary telangiectasias represent localized collections of dilated capillary-like vessels interspersed within normal brain. (Fig. 19) These lesions comprise 4-12% of vascular malformations, and are usually small, asymptomatic, incidental findings, although there are rare reports of symptoms including hemorrhage, seizure, vertigo, tinnitus, and cranial nerve dysfunction.[51] There is one reported case of a malignant fatal progression.[52] The etiology of these lesions is unclear, but it is hypothesized that they are acquired lesions secondary to underlying venous anomalies.[53] Most are located in the pons, but other common locations include the temporal lobe, medulla, or caudate. They are usually small, but in a small number of cases, they may exceed 1 cm in size.[51] The majority are solitary lesions, but they can be multiple in syndromes such as Osler-Weber Rendu, ataxia telangiectasia, or Sturge Weber. Unlike other vascular malformations of the brain, there is no reported calcification, gliosis or hemosiderin laden macrophages in the adjacent brain on microscopic exam.[51]

Capillary telangiectasias are not visible on CT imaging. MR imaging may reveal a focal area of T2 hyperintensity that on post-contrast imaging reveals ill-defined enhancement described as having a "stippled" or "brush stroke" appearance. An enlarged vessel is seen adjacent to these lesions in approximately two-thirds of cases, thought to represent a draining vein.[54] T2* imaging reveals associated low signal thought to reflect the presence of deoxyhemoglobin due to sluggish blood flow through the region.[55] (Fig. 20) There is no

associated mass effect. These lesions are occult on angiography, which may reflect sluggish flow, hemorrhage within the lesion, or abnormal vessels of small size.[51]

Figure 19. Capillary telangiectasia. Photograph of a gross specimen demonstrates dilated capillaries within the central aspect of the pons.

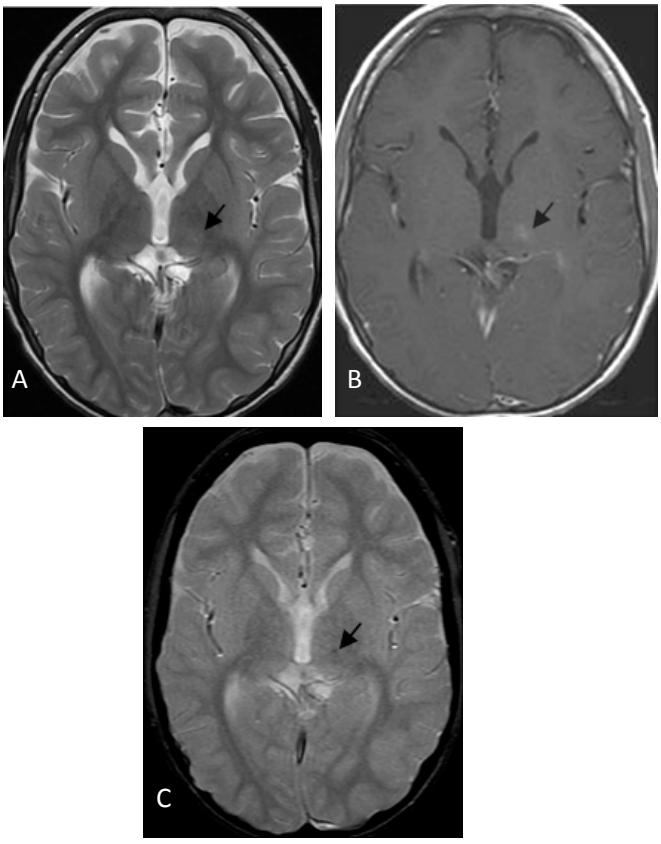

Figure 20. Capillary telangiectasia. (A) Axial T2-weighted image demonstrates a faint area of hyperintensity in the left thalamus (arrow). (B) Axial T1 post contrast reveals a "stippled" enhancement pattern (arrow). (C) T2* demonstrates a faint area of low signal within the lesion (arrow).

Unfortunately, these lesions may be mistaken for a more aggressive process, such as glial neoplasm. Location, low signal on T2*, enhancement, and lack of mass effect help support the diagnosis of capillary telangiectasia. A study by Finkenzeller, et al. found that these lesions also have a low signal on DWI, and they suggest utilizing this finding to help increase diagnostic accuracy.[55] Most are small and are monitored over time. No treatment is required.

Summary

There are a variety of vascular malformations of the CNS. Some of these are aggressive, high flow lesions and have a risk of hemorrhage or other complications; others behave in a more benign manner. Knowledge of the imaging findings of these lesions, along with the findings that might indicate which ones may hemorrhage or have other associated poor outcomes, aids in making treatment decisions.

The views expressed in this material are those of the author, and do not reflect the official policy or position of the U.S. Government, the Department of Defense, or the Department of the Air Force.

References

1. Geibprasert, S., et al., Radiologic assessment of brain arteriovenous malformations: what clinicians need to know. Radiographics. 30(2): p. 483-501.
2. Matsubara, S., et al., Angiographic and clinical characteristics of patients with cerebral arteriovenous malformations associated with hereditary hemorrhagic telangiectasia. AJNR Am J Neuroradiol, 2000. 21(6): p. 1016-20.
3. Hofmeister, C., et al., Demographic, morphological, and clinical characteristics of 1289 patients with brain arteriovenous malformation. Stroke, 2000. 31(6): p. 1307-10.
4. Al-Shahi, R. and C. Warlow, A systematic review of the frequency and prognosis of arteriovenous malformations of the brain in adults. Brain, 2001. 124(Pt 10): p. 1900-26.
5. Khaw, A.V., et al., Association of infratentorial brain arteriovenous malformations with hemorrhage at initial presentation. Stroke, 2004. 35(3): p. 660-3.
6. Marks, M.P., et al., Intranidal aneurysms in cerebral arteriovenous malformations: evaluation and endovascular treatment. Radiology, 1992. 183(2): p. 355-60.
7. Weerakkody, R.A., et al., Arteriovenous malformations. Br J Neurosurg, 2009. 23(5): p. 494-8.
8. Mullan, S., et al., Embryological basis of some aspects of cerebral vascular fistulas and malformations. J Neurosurg, 1996. 85(1): p. 1-8.
9. Lasjaunias, P., A revised concept of the congenital nature of cerebral arteriovenous malformations. Interv Neuroradiol, 1997. 3(4): p. 275-81.

10. Stevens, J., et al., De novo cerebral arteriovenous malformation: case report and literature review. AJNR Am J Neuroradiol, 2009. 30(1): p. 111-2.
11. Davidson, A.S. and M.K. Morgan, The embryologic basis for the anatomy of the cerebral vasculature related to arteriovenous malformations. J Clin Neurosci. 18(4): p. 464-9.
12. Jabbour, M.N., et al., Aberrant angiogenic characteristics of human brain arteriovenous malformation endothelial cells. Neurosurgery, 2009. 64(1): p. 139-46; discussion 146-8.
13. Kiroglu, Y., et al., Intracranial calcifications on CT. Diagn Interv Radiol. 16(4): p. 263-9.
14. Soderman, M., G. Rodesch, and P. Lasjaunias, Transdural blood supply to cerebral arteriovenous malformations adjacent to the dura mater. AJNR Am J Neuroradiol, 2002. 23(8): p. 1295-300.
15. Halim, A.X., et al., Longitudinal risk of intracranial hemorrhage in patients with arteriovenous malformation of the brain within a defined population. Stroke, 2004. 35(7): p. 1697-702.
16. Hamilton, M.G. and R.F. Spetzler, The prospective application of a grading system for arteriovenous malformations. Neurosurgery, 1994. 34(1): p. 2-6; discussion 6-7.
17. Newton, T.H. and S. Cronqvist, Involvement of dural arteries in intracranial arteriovenous malformations. Radiology, 1969. 93(5): p. 1071-8.
18. Merzoug, V., et al., Dural sinus malformation (DSM) in fetuses. Diagnostic value of prenatal MRI and follow-up. Eur Radiol, 2008. 18(4): p. 692-9.
19. Morales, H., et al., Documented development of a dural arteriovenous fistula in an infant subsequent to sinus thrombosis: case report and review of the literature. Neuroradiology. 52(3): p. 225-9.
20. Hai, J., et al., A dural arteriovenous fistula in cavernous sinus developed from viral meningitis. Acta Neurol Belg. 111(2): p. 146-8.
21. Cohen, S.D., et al., Dural arteriovenous fistula: diagnosis, treatment, and outcomes. Laryngoscope, 2009. 119(2): p. 293-7.
22. Davies, M.A., et al., The natural history and management of intracranial dural arteriovenous fistulae. Part 2: aggressive lesions. Interv Neuroradiol, 1997. 3(4): p. 303-11.
23. Cognard, C., et al., Cerebral dural arteriovenous fistulas: clinical and angiographic correlation with a revised classification of venous drainage. Radiology, 1995. 194(3): p. 671-80.
24. Jacobson, B.E., et al., Traumatic indirect carotid-cavernous fistula: report of two cases. Neurosurgery, 1996. 39(6): p. 1235-7; discussion 1237-8.
25. Kiyosue, H., et al., Treatment of intracranial dural arteriovenous fistulas: current strategies based on location and hemodynamics, and alternative techniques of transcatheter embolization. Radiographics, 2004. 24(6): p. 1637-53.
26. Raybaud, C.A., C.M. Strother, and J.K. Hald, Aneurysms of the vein of Galen: embryonic considerations and anatomical features relating to the pathogenesis of the malformation. Neuroradiology, 1989. 31(2): p. 109-28.
27. Hoang, S., et al., Vein of Galen malformation. Neurosurg Focus, 2009. 27(5): p. E8.
28. Gatscher, S., et al., Multislice spiral computed tomography for pediatric intracranial vascular pathophysiologies. J Neurosurg, 2007. 107(3 Suppl): p. 203-8.
29. Gailloud, P., et al., Diagnosis and management of vein of galen aneurysmal malformations. J Perinatol, 2005. 25(8): p. 542-51.
30. Dowd, C.F., et al., Transfemoral venous embolization of vein of Galen malformations. AJNR Am J Neuroradiol, 1990. 11(4): p. 643-8.
31. Gailloud, P., et al., Confirmation of communication between deep venous drainage and the vein of galen after treatment of a vein of Galen aneurysmal malformation in an infant presenting with severe pulmonary hypertension. AJNR Am J Neuroradiol, 2006. 27(2): p. 317-20.
32. Lasjaunias, P.L., et al., The management of vein of Galen aneurysmal malformations. Neurosurgery, 2006. 59(5 Suppl 3): p. S184-94; discussion S3-13.
33. Moriarity, J.L., R.E. Clatterbuck, and D. Rigamonti, The natural history of cavernous malformations. Neurosurg Clin N Am, 1999. 10(3): p. 411-7.
34. Batra, S., et al., Cavernous malformations: natural history, diagnosis and treatment. Nat Rev Neurol, 2009. 5(12): p. 659-70.
35. Li, D.Y. and K.J. Whitehead, Evaluating strategies for the treatment of cerebral cavernous malformations. Stroke. 41(10 Suppl): p. S92-4.
36. Scott, R.M., et al., Cavernous angiomas of the central nervous system in children. J Neurosurg, 1992. 76(1): p. 38-46.
37. Robinson, J.R., Jr., et al., Factors predisposing to clinical disability in patients with cavernous malformations of the brain. Neurosurgery, 1993. 32(5): p. 730-5; discussion 735-6.
38. Del Curling, O., Jr., et al., An analysis of the natural history of cavernous angiomas. J Neurosurg, 1991. 75(5): p. 702-8.
39. Clatterbuck, R.E., et al., Ultrastructural and immunocytochemical evidence that an incompetent blood-brain barrier is related to the pathophysiology of cavernous malformations. J Neurol Neurosurg Psychiatry, 2001. 71(2): p. 188-92.
40. Ruiz, D.S., H. Yilmaz, and P. Gailloud, Cerebral developmental venous anomalies: current concepts. Ann Neurol, 2009. 66(3): p. 271-83.
41. Dillon, W.P., Cryptic vascular malformations: controversies in terminology, diagnosis, pathophysiology, and treatment. AJNR Am J Neuroradiol, 1997. 18(10): p. 1839-46.
42. San Millan Ruiz, D. and P. Gailloud, Cerebral developmental venous anomalies. Childs Nerv Syst. 26(10): p. 1395-406.
43. Rothbart, D., et al., Expression of angiogenic factors and structural proteins in central nervous system vascular malformations. Neurosurgery, 1996. 38(5): p. 915-24; discussion 924-5.
44. Kondziolka, D., L.D. Lunsford, and J.R. Kestle, The natural history of cerebral cavernous malformations. J Neurosurg, 1995. 83(5): p. 820-4.
45. Abdulrauf, S.I., M.Y. Kaynar, and I.A. Awad, A comparison of the clinical profile of cavernous malformations with and without associated venous malformations. Neurosurgery, 1999. 44(1): p. 41-6; discussion 46-7.
46. Duffau, H., et al., Early radiologically proven rebleeding from intracranial cavernous angiomas: report of 6 cases and review of the literature. Acta Neurochir (Wien), 1997. 139(10): p. 914-22.
47. Sarwar, M. and W.F. McCormick, Intracerebral venous angioma. Case report and review. Arch Neurol, 1978. 35(5): p. 323-5.
48. Uchino, A., et al., Double cerebral venous angiomas: MRI. Neuroradiology, 1995. 37(1): p. 25-8.
49. Huber, G., et al., Regional association of developmental venous anomalies with angiographically occult vascular malformations. Eur Radiol, 1996. 6(1): p. 30-7.
50. San Millan Ruiz, D., et al., Parenchymal abnormalities associated with developmental venous anomalies. Neuroradiology, 2007. 49(12): p. 987-95.

51. Sayama, C.M., et al., Capillary telangiectasias: clinical, radiographic, and histopathological features. Clinical article. J Neurosurg. 113(4): p. 709-14.
52. Huddle, D.C., J.C. Chaloupka, and V. Sehgal, Clinically aggressive diffuse capillary telangiectasia of the brain stem: a clinical radiologic-pathologic case study. AJNR Am J Neuroradiol, 1999. 20(9): p. 1674-7.
53. McCormick, P.W., et al., Cerebellar hemorrhage associated with capillary telangiectasia and venous angioma: a case report. Surg Neurol, 1993. 39(6): p. 451-7.
54. Barr, R.M., W.P. Dillon, and C.B. Wilson, Slow-flow vascular malformations of the pons: capillary telangiectasias? AJNR Am J Neuroradiol, 1996. 17(1): p. 71-8.
55. Finkenzeller, T., et al., Capillary telangiectasias of the pons. Does diffusion-weighted MR increase diagnostic accuracy? Eur J Radiol. 74(3): p. e112-6.

Subdural Hemorrhage in Abusive Head Trauma: Imaging Challenges and Controversies

Gary L. Hedlund, D.O.

Division of Neuroimaging, Primary Children's Medical Center, Salt Lake City, UT

Background of abusive head trauma

In the neonate, infant, or young child who has suffered from non-accidental injury, abusive head trauma (AHT) is acknowledged as the most common cause of fatality and long term morbidity with approximately 1,500 fatalities and 18,000 seriously disabled infants and children annually in the USA.[1-4] Ninety-five percent of serious CNS injuries among infants less than 1 year of age are attributed to AHT.[2] Up to 80% of fatal child abuse injuries are attributed to head injury.[2] Unfortunately, most authors agree that these statistics represent an underestimation of this national health problem. Beyond the tragedy of an injured or murdered child is the broader social and community impact of this national and international health blight. In addition to the emotional, family, and social costs caused by inflicted trauma, the societal financial burden is astounding. In 2008, in the United States, costs ascribed to child abuse were estimated at 103 billion dollars; $33 billion for immediate intervention services and $70 billion for long-term costs.[5]

Subdural hemorrhage: a marker of pediatric head trauma

Subdural hemorrhage (SDH) is the most common pathology associated with abusive head trauma.[6-8] The historical teaching describing the origin and location of subdural hemorrhage has been that the tearing of bridging veins leads to bleeding at the interface between the inner (meningeal layer) dural margin and the arachnoid membrane.[9] This explanation does not completely reflect the potential sites of subdural compartment hemorrhage. More recently, Julie Mack and colleagues have advanced our understanding of a more dynamic vascularized dura.[10] They describe the inner dural border zone region (inner meningeal dura) as a location where loose intercellular junctions exist, possesses a vascularized layer, and represents the location of subdural compartment (intradural) hemorrhage. Hemorrhage in this location conforms to the classic morphology of subdural bleeding (concavoconvex). The authors also point out that in the first two years of life, the inner dural border zone plays an important role in the resorption of CSF as the arachnoid granulations are maturing.[10] This expanded discussion of the inner dura, hemorrhage origin, and hemorrhage location gives guidance to the medical imaging physician to describe bleeding in this location as subdural compartment hemorrhage. Of course, from the brain CT or MRI examinations which depict intracranial hemorrhage the intent behind trauma cannot be inferred. It is only after a comprehensive child protection team evaluation that the determination of abusive versus accidental or non-traumatic causes of hemorrhage is determined.

Imaging goals in the evaluation of abusive head trauma

The goals for the medical imaging physician who is responsible for interpreting brain CT and MRI examinations for the pediatric patient with suspected abusive head trauma are clearly defined. These include: the determination of findings that require urgent and emergent treatment, fully assessing the extent of injury, estimating the timing of injury, detecting intracranial injuries in abused children who present with clinical manifestations of extracranial injury, and detecting mimics of SDH and underlying conditions which predispose to non-traumatic SDH.[1,2,4,7]

CT is the examination of choice in the initial evaluation of pediatric head trauma. Its availability, rapid examination times, and sensitivity for detecting intracranial hemorrhage, early herniation patterns, and fractures make it an indispensible tool.[1,2,7] Additionally, if vascular injury is suspected, intravenous contrast enhanced CT angiography and venography can be accomplished with ease. CT lacks sensitivity in the detection of cortical contusion, early edema, infarction, shear-strain

injury (diffuse axonal injury), and subtle petechial hemorrhage.[1,2]

Brain MRI yields full appraisal of intracranial hemorrhage, parenchymal injury, signs of early herniation, and vascular complications including stroke and vessel dissection. In addition to spin magnitude imaging (including gradient recall imaging [GRE] or susceptibility weighted imaging [SWI] and diffusion weighted imaging [DWI]) which represents the minimum standard examination for trauma, MR adjuncts such as magnetic resonance spectroscopy (MRS), perfusion MR imaging (pMRI), and vascular adjuncts including MRA and MRV may contribute useful diagnostic information.[1,2,8] At our pediatric medical center, brain MRI is performed for all pediatric patients suspected of having inflicted head trauma with abnormal CT examinations, the pediatric patient suspected of being abused with encephalopathy and focal neurological signs regardless of the CT findings, and for the infant with extracranial manifestations of abuse. From a timing standpoint, we strive to accomplish the MR examination 3 to 5 days following presentation. This allows for optimal patient stabilization and expression of intracranial injuries.[1,2,7,8]

Dating intracranial hemorrhage using CT and MRI

Estimating the age of intracranial hemorrhage provides critical forensic information for the investigation of suspected abusive head trauma. I have found that CT and MRI findings are complementary when it comes to tackling the dating of an injury and characterization of intracranial hemorrhage. However, pinpointing the precise age of extraaxial hemorrhage is fraught with pitfalls and frankly, is unrealistic.[2,7,11,12] There are many factors that influence the CT and MRI appearance of subdural blood including the hemoglobin state, clot-serum separation, presence of an arachnoid tear with admixture of CSF and blood, RBC hydration, and MR technical considerations including magnetic field strength and the selection of scanning sequences.[13] The CT appearance of aging subdural hemorrhage is outlined in Table 1; this data represents a practical working tool for assessing the age of extraaxial hemorrhage. Here, a word of caution is in order. Note from Table 1, that the isodense appearance of hemorrhage could either represent hyperacute blood or early subacute hemorrhage.[14] Also, the patient with an acute SDH and a hemoglobin value of < 8 g/dl will exhibit an isodense hemorrhage.[13,14] Therefore, when the interpreting radiologist is assessing the initial CT examination the impression of the CT findings should be descriptive; emphasizing the appearance or density features of the hemorrhage rather than emphasizing the stage of hemorrhage (Table 1). Here is where an argument can be made for a short interval repeat CT examination (within 24 to 48 hours of the initial study) to clarify hypodense or isodense subdural components.

CT Evolution of Subdural Hemorrhage (SDH)	
≤ 3 Hours	Iso-to-Hypoattenuating
Few Hours → 7-10 Days	Hyperattenuating
2-3 Weeks	Isoattenuating
> 3 Weeks	Hypoattenuating

Table 1. (Modified from Reference 7)

Using MR as a means of dating subdural hemorrhage is even more complex than CT dating for reasons mentioned above. Although the work by Bradley has laid a foundation for our understanding of the MR evolution of intracranial hemorrhage, it must be kept in mind that the MRI evolutionary findings of intracranial hemorrhage are observations drawn from intraparenchymal hematoma aging (Table 2).[13] The relatively elevated parenchymal levels of tissue thromboplastin and higher tissue oxygen tension lead to more rapid degradation of blood than found within extraaxial hemorrhage.[13,15] Given this information, as medical imaging physicians, we must use the MRI guidelines for hemorrhage evolution as a dating estimate and always interpret MRI in conjunction with CT observations.[8]

Mixed density subdural hemorrhage

Interpretation of the mixed density subdural hemorrhage can be a source of confusion and inaccuracy when interpreting brain imaging.[2,7,8] Historically, dogma has stated that mixed density SDH represents a combination of new and old

Evolution of Intraparenchymal Hematoma – MRI				
Stage	Age	T1WI	T2WI	Hb State
Hyperacute	< 12-24 hours	Iso– to – Hypo	Hyper	Oxy-Hb
Acute	1-3 Days	Hypo	Very Hypo	Deoxy – Hb (Ic)
Early Subacute	2-3 Days → 1-2 wks	Very Hyper	Very Hypo	Met – Hb
Late Subacute	1-2 wks → 1-2 mo	Very hyper	Very Hyper	Met – Hb(Ec)
Chronic	Few wks → mos/yrs	Iso	Very Hypo	Hemosiderin (SD membrane)
Chronic	Few wks → mos/yrs	Hypo	Hyper	Nonparamagnetic hemochromes (SD content)

Key: Ic = Intracellular, Ec = extracellular, SD = subdural

Table 2. (Modified from reference 7)

blood. Four diagnostic considerations should come to mind for the radiologist in the setting of mixed density SDH. These include: hyperacute + acute blood, acute hemorrhage alone, hematohygroma (acute hemorrhage + CSF secondary to arachnoid tear), and the combination of new and old hemorrhage.[2,7,8] The first three examples of mixed density SDH can derive from a single traumatic event (Fig 1). In my experience, the mixed density SDH associated with ipsilateral cerebral edema is usually associated with one of the first three causes. Tung and colleagues reported that SDH in the context of abusive head trauma was more likely to be mixed density, bilateral in location, contrecoup, and affiliated with poor neurological outcome. SDH of accidental cause was more homogeneous, unilateral and coup to the site of impact (Fig 2).[16] Hymel and colleagues have also reported their CT observations in pediatric accidental and abusive head trauma.[17] A sediment or hematocrit layer may be seen shortly after trauma and may result from one traumatic event. For purposes of dating, the radiologist should focus upon the CT and MR features of the sediment for most accurately estimating hemorrhage age (Fig 3).[12]

The presence of membranes within the subdural hemorrhage is very helpful to strengthen the radiologist's diagnostic confidence of new and old subdural blood. Delicate incomplete membranes begin to form within the subdural hemorrhage within 2 to 3 weeks and mature by 4 to 5 weeks.[18,19] CT can suggest the presence of membranes but MR provides the most information regarding membrane structure and signal intensity (Fig 4). Membrane detection requires careful inspection of all pulse sequences. With older membranes, GRE and/or SWI will be helpful in detection. Membrane conspicuity may be heightened by the use of intravenous MR

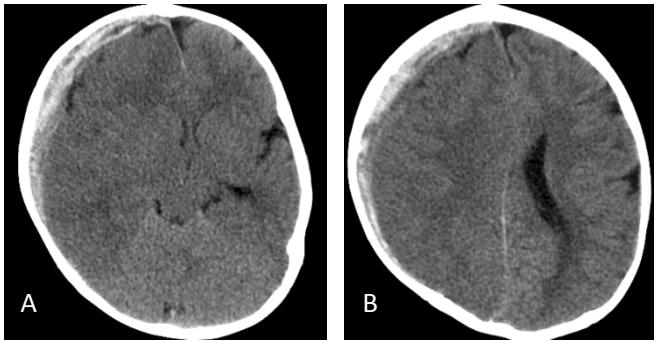

Figure 1: Mixed density subdural hemorrhage. (A). Non-contrast CT through the level of the frontal horns shows a heterogeneous right frontotemporal SDH. Note the associated right hemispheric cerebral edema and subfalcine herniation. (B). Non-contrast CT through the cerebral convexities demonstrates the cephalad extent of the subdural bleed and early obstruction of the left lateral ventricle due to compression at the left foramen of Monro as a result of the subfalcine herniation. At surgery the hemorrhage was all found to be acute. The perpetrator confessed to grasping the infant's neck and shaking.

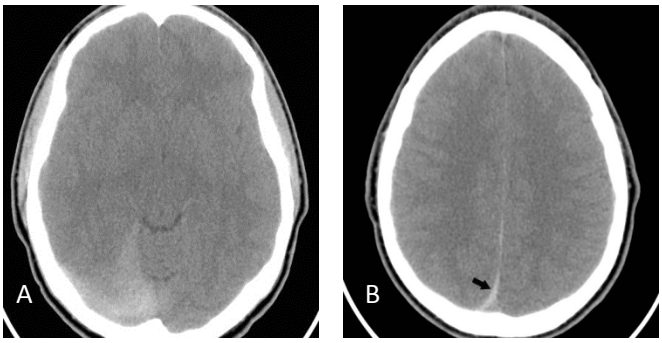

Figure 2: Accidental subdural hemorrhage. (A). Non-contrast CT shows a homogeneous increased attenuation SDH involving the right tentorium. (B). A small posterior parafalcine component of the SDH is also noted (arrow). This fifteen-year-old female had accidental closed head trauma ipsilateral to the SDH.

contrast and post-contrast T1 weighting and subtraction MR imaging techniques.[1,2,7]

Re-bleeding into subdural hemorrhage

Re-bleeding into a subdural hemorrhage remains a controversial topic and when observed brings to mind concern over whether the new blood represents: spontaneous hemorrhage, bleeding due to minimal trauma, or hemorrhage secondary to major trauma.[2,20] The corresponding clinical picture at the time of presentation is very important to consider as the encephalopathic child with new subdural hemorrhage is much more likely to have experienced significant trauma.[20] A careful child

protection team evaluation is warranted in this setting to determine if physical abuse is the likely cause of the new imaging findings. Additionally, the radiologist should always keep in the back of his or her mind the possibility of non-traumatic causes of SDH and re-bleeding (as one might see with a progressive neurodegenerative disorder) (Table 3).

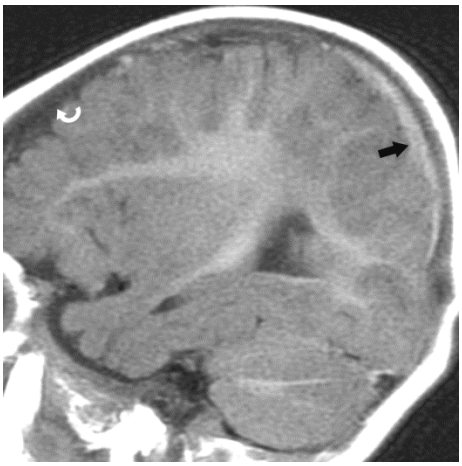

Figure 3: Early subacute subdural hemorrhage with sediment. Parasagittal T1 weighted MR image shows a thin parietooccipital hyperintense subdural hemorrhage (arrow). Note the thin hypointense frontal subdural fluid (curved arrow). The perpetrator confessed to three strong shaking episodes four days prior to the MRI. The redistribution of hemorrhage can occur within hours of the insult. For dating, the radiologist should focus attention upon the sediment.

Mimics and Non-Traumatic Causes of Subdural Hemorrhage

- Coagulopathies: vitamin K deficiency
- Hematologic disorders: leukemia, hemophilia
- Arachnoid cyst
- Vascular: aneurysm, arteriovenous malformation, dural AVF
- Meningitis
- Metabolic: glutaric aciduria type 1, galactosemia, pyruvate carboxolase deficiency
- Neoplasms: leukemia, leptomeningeal PNET, leptomeningeal melanoma
- Neoplastic like : hemophagocytic lymhohistiocytosis
- Other: Menkes disease

Table 3. (Modified from Reference 2)

Birth related subdural hemorrhage

Birth related SDH can lead to confusion and controversy particularly when SDH is detected in a young infant.[21] In a recent article by Rooks and colleagues, 101 asymptomatic newborns were studied with cranial sonography and MRI. The prevalence of SDH in their population was 46%. Take home points from their paper were that SDH was most common in the parietooccipital and tentorial locations, thin SDH (most < 3 mm in thickness), and nearly all SDHs had resolved by one month of life (Fig 5). Additionally, in the first three days of life, hemorrhage was most accurately detected with gradient recall imaging (GRE) at a time when acute hemorrhage was isointense on T1 weighted images.[22]

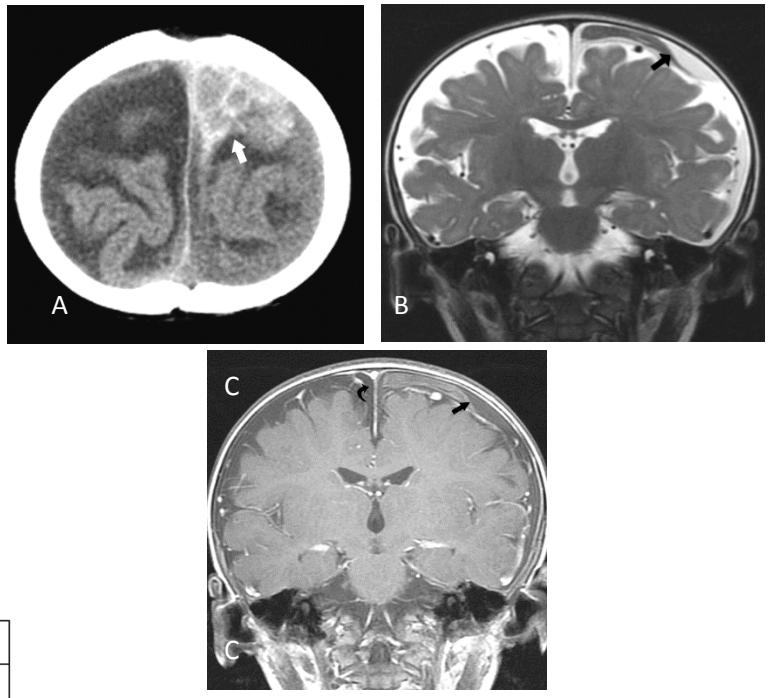

Figure 4: Membrane formation within subdural hemorrhage. (A). NCCT showing a heterogeneous left parafalcine subdural hemorrhage (arrow). This hemorrhage had been interpreted as an acute bleed at the referring hospital. (B). Coronal T2 weighted MR image shows a sharp transition (arrow) between the medial hypointense hemorrhage (early subacute) and lateral hyperintense to cortex (early chronic) subdural hemorrhage. (C). Coronal T1 weighted MR image with IV contrast shows T1 shortening (enhancement) within the subdural membrane (arrow). Also note the small T1 hypointense (chronic) right parafalcine subdural hemorrhage (curved arrow). Well defined membranes within subdural hemorrhages take 4 to 6 weeks to form.

Subdural hemorrhage with benign expanded subarachnoid spaces

Benign expanded subarachnoid spaces represent a common finding among infants with

macrocephaly who are otherwise normal. The etiology of these collections likely represents a transient mismatch between CSF production and resorption.[23,24] In the first two years of life, the arachnoid granulations are undergoing maturation. Additionally, during infancy, the inner dural border zone may play an important role in CSF resorption at a time of evolving arachnoid granulation maturation.[10]

When evaluating prominent extracerebral collections and considering the diagnosis of benign subarachnoid fluid, the radiologist should look for clues that allow assignment of the of the fluid to the subarachnoid space and thus exclude subdural compartment collections.[24] These findings include: visualization of corticodural veins traversing the fluid (positive cortical vein sign), interdigitation of the fluid into the cortical sulci, symmetry of the fluid interface with the dura, and iso-attenuation (CT) or isointensity (MRI) features of the fluid on imaging studies.[25]

Controversy arises when SDH is detected in association with these expanded subarachnoid spaces (Fig 6). There are authors who posit that in the context of benign expanded subarachnoid spaces that SDH can occur spontaneously or with minimal trauma.[26-30] My experience over twenty years of interpreting pediatric neuroimaging studies is that the occurrence of SDH with benign expansion of the subarachnoid spaces without a history of trauma is a rare event. Therefore, in my clinical practice, the detection of SDH in association with benign expanded subarachnoid CSF collections warrants a comprehensive child protection team evaluation.

Subdural hemorrhage and intracranial venous thrombosis

In the differential diagnostic consideration of non-traumatic causes of SDH, some authors opine and testify to the fact that intracranial venous thrombosis (ICVT) may lead to the development of SDH that mimics the SDH of abusive head trauma.[4,31,32] At the 2011 American Society of Neuroradiology (ASNR) meeting in Seattle Washington, Dr Logan McClain and colleagues reported their observational retrospective CT and MRI study of 36 pediatric patients with non-traumatically acquired intracranial venous thrombosis, looking for the presence of SDH. None of the 36 were found to have SDH [AJNR In Press]. Of course, trauma can be a cause for ICVT and subdural hemorrhage alike.

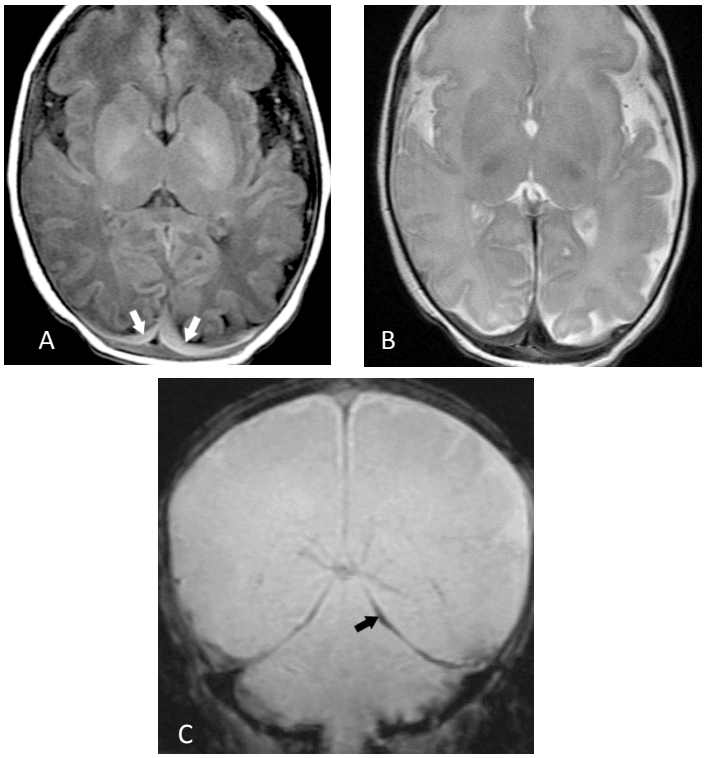

Figure 5: Birth related subdural hemorrhage in a four-day-old newborn. (A). Axial T1 weighted image shows bilateral thin occipital hyperintense subdural hemorrhages (arrows); typical for size and location of birth related subdural hemorrhages. (B). Axial T2 weighted MR image shows these subdural bleeds to be hypointense (early subacute). (C). Coronal gradient recall (GRE) (T2*) MR image shows the presence of a thin left tentorial subdural hemorrhage (arrow). This is also a common location for birth related SDH. GRE images are particularly helpful in the first few days following birth when the T1 signal intensity of birth related hemorrhage will be isointense.

Hypoxic ischemic encephalopathy and subdural hemorrhage

Finally, there has been recent controversy raised over whether hypoxic ischemic encephalopathy (HIE) is a potent cause of SDH which may mimic the features of abusive head trauma.[33,34] In my experience and in that of other authors, HIE may certainly accompany other findings consistent with abusive head trauma. Of course, child birth related subdural hemorrhage may occur in conjunction with HIE without a causal relationship. Several large

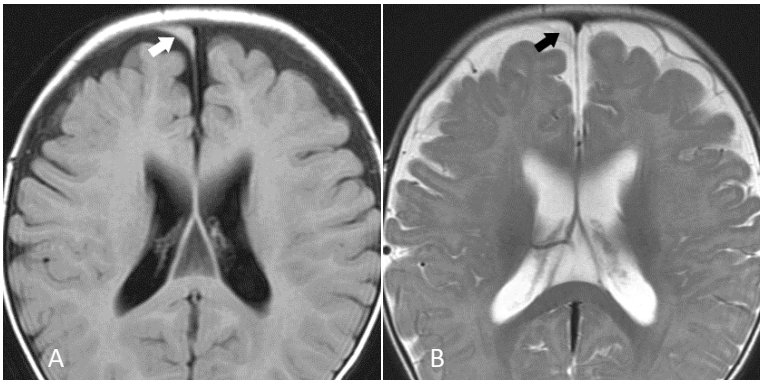

Figure 6: Subdural hemorrhage in the setting of macrocrania and benign expansion of the subarachnoid spaces. (A). Axial T2 fluid attenuated inversion recovery image (FLAIR) shows a small slightly hyperintense right parafalcine frontal subdural hemorrhage (arrow). (B). Axial T2 MR image shows heterogeneity of the SDH (arrow) and hypointense cortical veins coursing through the expanded subarachnoid spaces (positive cortical vein sign).

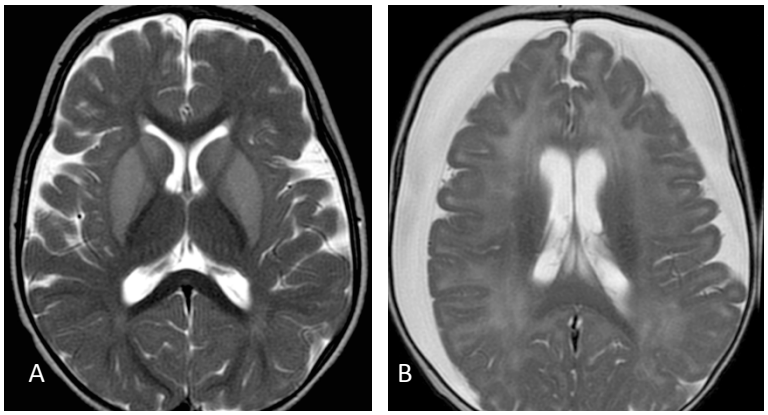

Figure 7: Glutaric aciduria type I. A non-traumatic cause of SDH (A). Axial T2 weighted MR image in a child with the metabolic disorder of glutaric aciduria type I shows bilateral basal ganglia swelling and hyperintensity. These regions also showed evidence for cytotoxic edema on diffusion weighted MR imaging. (B). Six months later, new onset seizures prompted a repeat MRI. The T2 MR image shows the interval development of large chronic subdural hemorrhages. Brain parenchymal volume loss (due to nueodegeneration) was confirmed on other sequences. When subdural collections are detected, the radiologist must closely inspect the brain parenchyma for signs of atrophy.

non-traumatic observational patient cohort studies have failed to substantiate HIE as a cause of SDH.[35]

Non-traumatic causes of subdural hemorrhage

Finally In addition to the key observations that the radiologist must make in the setting of suspected abusive head trauma, there must be an awareness that some disorders may either as a result of mechanical distortion or neurodegeneration predispose to the development of non-traumatic SDH (Table 3).[36-42] To avoid this pitfall, the radiologist must be alert to key clinical features, laboratory abnormalities, and imaging clues that suggest an underlying cerebral parenchymal disorder (Fig 7).[36-42] Of course, a comprehensive clinical, and laboratory evaluation of the patient with a chronic neurologic disorder and SDH is mandatory. It is worth remembering that physical abuse is more common among children with chronic illness.[43]

Reporting responsibilities for the radiologist when AHT is suspected

The radiologist shoulders an important responsibility when it comes to reporting imaging findings suggesting abusive head trauma. The law is clear in this regard. For the radiologist, there is a legal responsibility to report findings suspicious for AHT. These guidelines are outlined by the American College of Radiology, and can be reviewed at (www.acr.org/guidelines). Documentation of the individual contacted, the method of communication, the date and time are minimal requirements. As a mandatory reporter, the radiologist is protected from civil and criminal prosecution by Shield Laws that exist within the United States. The radiologist should inquire with their local child protection team and/or county medical association to review specific state statutes.

References

1. Hedlund GL, Frasier LD. Neuroimaging of abusive head trauma. Forensic Sci Med Pathol, Springer Science Business Media 2009.
2. Medina LS, et al. Imaging of nonaccidental head injury. Evidence-Based Imaging in Pediatrics 2010; 12:161.
3. Fernando S, Obaldo Ruby, Walsh I, Lowe L. Neuroimaging of nonaccidental head trauma; pitfalls and controversies. Pediatric Radiol 2008; 38: 827-838.
4. Barnes P, Krasnokutsky M. Imaging of the CNS in Genetic Mimics Suspected or Alleged NAI. Top Magn Reson Imaging 2007; 18:53-74.
5. Wang CT, Holton J. Total estimated cost of child abuse neglect in the United States. Prevent Child Abuse America Web site. Updated Sept. 2007. Accessed Aug. 15, 2008.

6. Hoskote A, Richards P, Anslow P, et al. Subdural hematoma and non-accidental head injury in children. Child's Nervous System, 2002; 18:311-17.
7. Vezina G. Assessment of the nature and age of subdural collections in nonaccidental head injury with CT and MRI. Pediatric Radiol, 2009; 39:586-590.
8. Huisman TA. Intracranial hemorrhage: ultrasound, CT and MRI findings. Eur Radiol, 2005; 15:434-440.
9. Fobben E, Grossman R, Atlas Scott, Hackney David, Goldberg H, Zimmerman R, Bilaniuk L. MR characteristics of subdural hematomas and hygromas at 1.5 T. AJNR 1989; 10:687-693.
10. Nelson M. Unraveling the puzzle. Pediatric Radiol, 2009; 39:199.
11. Lee KS, Bae WK, Bae HG et al. The computed tomographic attenuation and the age of subdural hematomas. J Korean Med Sci 1997; 12:353-359.
12. Vinchon M, Noule' N, Tchofo P, Soto-Ares G, Fourier C, Dhellemmes P. Imaging of head injuries in infants: temporal correlates and forensic implications for the diagnosis of child abuse. J Neurosurg (Pediatrics 1) 2004; 101:44-52.
13. Bradley WG Jr, MR appearance of hemorrhage in the brain. Radiology 1993; 189:15-26.
14. Sargent S, Kennedy JG, Kaplan JA. "Hyperacute" subdural hematoma: CT mimic of recurrent episodes of bleeding in the setting of child abuse. J Forensic Sci. 1996; 41:314-316.
15. Williams VL, Hogg JP. Magnetic resonance in imaging of chronic subdural hematoma. Neurosurg Clin N Am. 2000; 11:491-498.
16. Tung GA, Kumar M, Richardson RC et al. Comparison of accidental and nonaccidental traumatic head injury in children on noncontrast computed tomography. Pediatrics. 2006; 118:626-633.
17. Hymel KP, Rumack CM, Hay TC et al. Comparison of intracranial computed tomographic findings in pediatric abusive and accidental head trauma. Pediatr Rad 1997; 27:743-747.
18. Munro D, Merritt H. Surgical pathology of subdural hematoma. Based on a study of 105 cases. Arch Neurol Psychiatr. 1936; 35:64-78.
19. Hanna JA. The aetiology of subdural hematoma: an anatomical and pathological study. J Nerv Ment Dis. 1936; 84:169-186.
20. Hymel K, Jenny C, Block R. Intacranial hemorrhage and rebleeding in suspected victims of abusive head trauma: addressing the forensic controversies. Child Maltreat 2002; 7:329-48.
21. Gupta SN, Kechli AM, Kanamalla US. Intracranial hemorrhage in term with newborns: management and outcomes. Pediatr Neurol 2009; 40:1-12.
22. Rooks VJ, Eaton JP, Ruess L et al. Prevalence and evolution of intracranial hemorrhage in asymptomatic term infants. AJNR 2008; 29:1082-1089.
23. Babock D, Han B, Dine M. Sonographic findings in infants with macrocrania. AJR 1988; 150:1359-1365.
24. Wilms G, Vanderschueren, Demaerel P, Smet M, Van Calenbergh F, Plets C, Goffin J, Casaer P. CT and MR in infants with pericerebral collections and macrocephaly: Benign enlargement of the subarachnoid spaces versus subdural collections. AJNR 1993; 14:855-860.
25. McCluney K, Ueakley J, Festermacher M, et al. Subdural hygroma versus atrophy on MR brain scans: "the cortical vein sign." AJNR 1992; 13:1335-1339.
26. Vinchon M, Delstret I, DeFoort-Dhellemmes S, Desurmont M, Noueleʼ N. Subdural hematoma in infants: can it occur spontaneously? Data from a prospective series and critical view of the literature. Child's Nerv Syst. Online Publication: 2010.
27. McNeely P, Atkinson J, Saigal G, O'Gorman A, Farmer J. Subdural hematomas in infants with benign enlargement of the subarachnoid spaces are not pathognomonic for child abuse. AJNR 2006; 27:1725-28.
28. Ravid S, Maytal J. External hydrocephalus: a probable cause for subdural hematoma in infancy. Pediatr Neurol 2003; 28:139-141.
29. Raul JS, Roth S, Ludes B et al. Influence of the benign enlargement of the subarachnoid space on the bridging veins strain during a shaking event: a finite element study. Int J Legal Med. 2008: 122:337-340.
30. Spektor Amodio, Pramanik B et al. Spontaneous development of bilateral subdural hematomas in an infant with benign infantile hydrocephalus: color Doppler assessment of vessels traversing extra-axial spaces. Pediatr Radiol 2005; 35:1113-1117.
31. Matsuda M, Matsuda I, Sato M, Handa J. Superior sagittal sinus thrombosis followed by subdural hematoma. Surg Neurol 1982; 18:206-11.
32. Takamura Y, Morimoto S, Uede T et al. Cerebral venous sinus thrombosis associated with systemic multiple hemangiomas manifesting as chronic subdural hematoma – case report. Neurol Med Chir (Tokyo) 1996; 36:650-3.
33. Cohen MC, Scheimberg I. Evidence of occurrence of intradural and subdural hemorrhage in the perinatal and neonatal period in the context of hypoxic ischemic encephalopathy. An observational study from two referral institutions in the United Kingdom. Pediatr Dev Pathol 2008; 36:92-96.
34. Geddes JF, Tasker RC, Hackshaw AK et al. Dural hemorrhage in non-traumatic infant deaths: does it explain the bleeding in 'shaken baby syndrome'? Neuropathol Appl Neurobiol. 2003; 29:14-22.
35. Hurley M, Wilson S, McConachie N, Dineen R, Padfield C, Stephenson T, Vyas H, Jaspan T. Is there a casual relationship between the hypoxia-ischemia associated with cardiorespiratory arrest and subdural hematomas? An observational study. The British Journal of Radiology. 2010; 83:736-43.
36. Sirotnak A. Medical disorders that mimic abuse head trauma. Abusive Head Trauma in Infants and Children. St. Louis (MO): GW Medical Publishing 2006; 191-196.
37. Ganesh A, Jenny C, Heter J, et al. Retinal hemorrhages in type I osteogenesis imperfect after minor trauma. Ophthalmology 2004; 111:1428-31.
38. Groniger A, Schaper J, Messing-Juenger M, et al. Subdural hematoma as clinical presentation of osteogenesis imperfecta. Pediatr Neurol 2005; 32:140-2.
39. Strauss K, Puffenberger E, Robinson D, et al. Type I glutaric aciduria part 1: natural history of 77 patients. Semin Med Genet 2003; 121:38-52.

40. Nassogne MC, Sharrad M, Hertz-pannier L, et al. Massive subdural hematomas in Menkes disease mimicking shaken baby syndrome. Childs Nerv Syst 2002; 18:729-31.
41. Ernst L, Sondheimer N, Deardorff M, et al. The value of the metabolic autopsy in the pediatric hospital setting. J Pediatr 2006; 148:779-83.
42. DeWolfe CC. Apparent life-threatening event: a review. Pediatr Clin North Am 2005; 52:1127-46.
43. Jaudes PK, et al. Child Abuse Neglect. E-pub 2008 Jul; 32(7): 671-81.

Vascular Retrotympanic Mass

Aaron Betts, M.D.,[a] Carlos Esquivel, M.D.,[b] and William T. O'Brien, Sr., D.O.[a]

[a] Department of Diagnostic Imaging, Wilford Hall Ambulatory Surgical Center, San Antonio, TX
[b] Department of Otolaryngology, Wilford Hall Ambulatory Surgical Center, San Antonio, TX

Case Presentation

A 45-year-old woman presented with a 3-year history of pulsatile tinnitus in her left ear. She denied hearing loss or otalgia. Past medical history and review of systems were noncontributory. Physical examination revealed a red mass behind the posterior aspect of the tympanic membrane. There was no middle ear effusion, tympanic membrane retraction, or tympanic membrane perforation. External auditory canal was normal in appearance. The patient was subsequently referred for both CT and MRI of the temporal bones and internal auditory canals, respectively, to evaluate for a vascular retrotympanic mass. (Fig.)

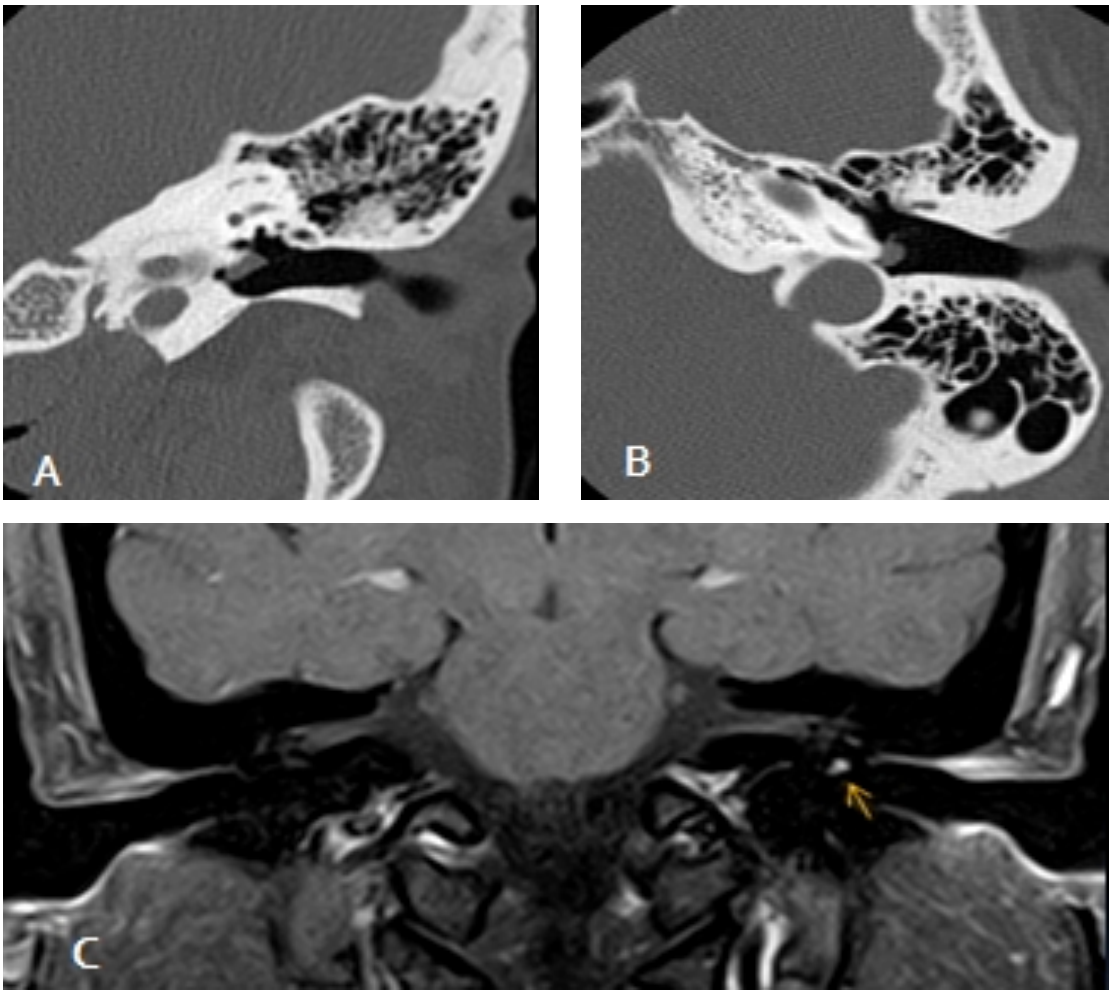

Figure. Coronal (a) and axial (b) CT images through the left temporal bone demonstrate a small, circumscribed soft tissue mass located within the middle ear along the cochlear promontory. Coronal T1 post-contrast fat suppressed MR image (c) reveals diffuse enhancement of the middle ear mass (arrow).

Key clinical finding(s)
Vascular retrotympanic mass

Key imaging finding(s)
Enhancing retrotympanic mass

Differential diagnoses
Glomus tympanicum
Variant vasculature
Cholesterol granuloma

Discussion
Tinnitus refers to abnormal ringing in the ears. It may be characterized as pulsatile or continuous and subjective or objective. Subjective tinnitus is perceived by the patient; objective tinnitus may be heard by others during physical examination. In the setting of tinnitus, the physical examination often guides the differential diagnosis and imaging work-up. If a vascular retrotympanic mass is identified on otoscopy, the primary differentials include a glomus tumor, variant vasculature, and cholesterol granuloma. The role of imaging is to exclude variant vasculature prior to biopsy or resection. MRI and CT often play complementary roles.

Glomus tympanicum: Glomus tympanicum is a paraganglioma which occurs within the middle ear adjacent to the cochlear promontory. It arises from glomus bodies along the course of Jacobson's nerve, which is a branch of the glossopharyngeal nerve. The tumor is of neural crest origin and is highly vascular. Clinically, patients present with pulsatile tinnitus, and a vascular retrotympanic mass is visualized on physical examination. Occasionally, patients may experience conductive hearing loss.[1]

On CT, glomus tympanicum presents as a soft tissue mass along the cochlear promontory with extension into the middle ear space. When large, it may be indistinguishable from other causes of middle ear opacification. The tumor typically does not result in significant ossicular or bony erosion. The MR appearance of glomus tympanicum depends on the size of the lesion. Smaller lesions are hyperintense on T2 sequences with avid enhancement on postcontrast T1 sequences. Larger lesions (greater than 10 mm) may show the characteristic "salt and pepper" appearance secondary to regions of hemorrhage (increased signal intensity) and a combination of flow voids and calcification (decreased signal intensity).[2]

Variant vasculature: A high riding internal jugular vein with or without dehiscence is the most common vascular variant affecting the temporal bone. The jugular vein is considered high riding if it extends above the inferior margin of the internal auditory canal. If the sigmoid plate separating the jugular vein from the middle ear cavity is dehiscent, a vascular retrotympanic mass may be seen on physical examination.

An aberrant internal carotid artery is a developmental abnormality which results from agenesis of the cervical and proximal petrous portions of the ICA. As a result, alternate anastamoses form via the external carotid artery. There is collateralization through the inferior tympanic artery (a branch of the ascending pharyngeal artery) to the caroticotympanic branch of the petrous ICA, both of which traverse the middle ear cavity. The enlarged caroticotympanic branch then anastamoses with the horizontal segment of the petrous ICA.[3] Cross-sectional imaging demonstrates narrowing and posterolateral deviation of the ICA into the middle ear cavity, along with absence of the cervical and proximal portion of the petrous ICA. Occasionally, a persistent stapedial artery may coexist with an aberrant ICA. Clinically, patients present with pulsatile tinnitus and a vascular retrotympanic mass, similar to a glomus tympanicum.

Cholesterol granuloma: Cholesterol granuloma occurs secondary to nonspecific chronic inflammatory changes and is most commonly seen in the petrous apex and middle ear cavity. Hemorrhage, cholesterol, and granulation tissue are the hallmarks of the lesion and account for its appearance on MR.[4] Patients most often present with conductive hearing loss and a vascular appearing retrotympanic mass on physical examination.

On CT, the imaging appearance is nonspecific with a soft tissue middle ear mass. Findings on MRI are more characteristic, demonstrating a nonenhancing middle ear mass which is hyperintense on both T1 and T2 sequences secondary to hemorrhagic blood products.[5] Care must be taken to compare pre and postcontrast T1 sequences, since the lesions are hyperintense on both which may be mistaken for enhancement. With adjacent inflammation, there may be thin peripheral enhancement.

Diagnosis

Glomus tympanicum

Summary

Cross-sectional imaging is an important component of the work-up and management of patients with tinnitus and a vascular retrotympanic mass. The primary role of imaging is to exclude variant vasculature as the cause of a retrotympanic mass prior to biopsy or resection. MRI and CT play complementary roles. Imaging findings are often characteristic for the clinical differential diagnoses, which include glomus tympanicum, variant vasculature, and cholesterol granuloma. Therefore, knowledge of these imaging patterns is essential when interpreting these studies.

The views expressed in this material are those of the author, and do not reflect the official policy or position of the U.S. Government, the Department of Defense, or the Department of the Air Force.

References

1. Remley KB, Coit WE, Harnsberger HR, et al. Pulsatile tinnitus and the vascular retrotympanic membrane: CT, MR, and angiographic findings. Radiology 1990; 174: 383-389.

2. Olsen WL, Dillon WP, Kelly WM, et al. MR imaging of paragangliomas. AJR Am J Roentgenol 1987; 148(1): 201-204.

3. Sauvaget E, Paris J, Kici S, et al. Aberrant internal carotid artery in the temporal bone: imaging findings and management Arch Otolaryngol Head Neck Surg 2006; 132: 86-91.

4. Moonis G, Kim A, Bigelow D, Loevner LA. Temporal bone vascular anatomy, anomalies, and disease, with an emphasis on pulsatile tinnitus. In: Swartz JD, Loevner LA. Imaging of the temporal bone, 4th ed. New York: Thieme; 2009: 289-91.

5. Martin N, Sterkers O, Mompoint D, et al. Cholesterol granulomas of the middle ear cavities: MR imaging. Radiology 1989; 172(2): 521-25.

Diffuse Cauda Equina Nerve Root Enhancement

Michael Zapadka, D.O.

Department of Diagnostic Imaging, Wake Forest University Baptist Medical Center, Winston-Salem, NC

Case Presentation

A 3-year-old otherwise healthy girl presented with a 7-day history of progressive bilateral lower extremity weakness. The patient had difficulty walking at the time of presentation. Past medical history was noncontributory. Review of systems revealed treatment for an upper respiratory system infection approximately 6 weeks prior to symptom onset. Physical exam revealed decreased strength in the bilateral lower extremities. She was otherwise neurologically intact. The patient subsequently underwent an MR examination of the lumbar spine with and without contrast. (Fig.)

Figure. Sagittal (a), coronal (b), and axial (c) T1 post contrast images with (a) and without (b and c) fat suppression demonstrate diffuse, smooth avid enhancement of the distal cord/conus and nerves roots of the cauda equina, which are mildly thickened.

Key imaging finding(s)

Diffuse cauda equina nerve root enhancement

Differential diagnoses

Gullain-Barré syndrome
Chronic inflammatory polyneuropathy
Arachnoiditis
Spinal meningitis
Leptomeningeal carcinomatosis

Discussion

Abnormal enhancement involving the spinal cord or the cauda equina carries a broad differential diagnosis, but the most common etiologies include infectious/inflammatory processes versus neoplastic or granulomatous diseases. Less common causes of nerve root enhancement include hereditary motor-sensory neuropathies (i.e. Charcot-Marie-Tooth syndrome and Dejerine-Sottas disease), Krabbe's disease and vasculitic neuropathies.[1] While CT and MR findings are often complementary, MRI is the imaging study of choice when evaluating a patient with extremity weakness, paresthesias or GI/GU dysfunction. While the imaging findings are often nonspecific, a clinical diagnosis is usually straightforward in the context of the patient's age, clinical history, CSF analysis and nerve conduction studies. However, imaging is a key component of the diagnostic workup to evaluate for the presence of nerve root enhancement, to establish an appropriate differential diagnosis and to assess patient's for treatment response.

Gullain-Barré syndrome:

Guillain-Barré syndrome (GBS) is an acute, monophasic inflammatory demyelinating polyneuropathy (AIDP) that is widely thought to be autoimmune in nature. More than 70% of patients report an antecedent event by 3 to 4 weeks including infection, vaccination or surgery.[2] GBS is the most common cause of acute flaccid paralysis worldwide, with an incidence of 1 to 3 per 100,000 persons.[3,4] Early symptoms of GBS include paresthesias of the lower extremities and low back pain which progresses to weakness or paralysis (usually symmetrically) with loss of tendon reflexes. There is typically little or no sensory disturbance.[4] Onset of weakness occurs within hours to days of symptom onset and may progress for up to four weeks.[4] Weakness generally begins in the lower extremities and classically progresses in an ascending manner with subsequent involvement of the upper extremities, cranial nerves and brainstem. Diagnosis is generally made by clinical history, physical exam and CSF analysis (increased protein without pleocytosis). There is no proven benefit from corticosteroid therapy and treatment options include plasmapheresis or intravenous gamma globulin with patients generally exhibiting clinical improvement by 2 months.

Imaging findings classically include smooth, avid enhancement of nerve roots of the cauda equina, often with preferential involvement of the ventral (motor) nerve roots.[5] Nerve roots may be thickened, but remain smooth in contour without nodularity. Additionally, there may be enhancement along the pial surface of the distal cord and conus medullaris, though the conus should be normal in size and without associated intramedullary signal abnormality. Improvement in imaging findings coincides with resolution of clinical symptoms.

Chronic inflammatory demyelinating polyneuropathy:

Chronic inflammatory demyelinating polyneuropathy (CIDP) is an acquired, immune-mediated mixed motor and sensory polyneuropathy. Patients present with predominantly motor symptoms, including symmetric weakness involving both proximal and distal muscles of the upper and lower extremities. In contrast to Guillain-Barré syndrome, an antecedent event is identified in less than 30% of patients with CIDP and symptoms progress over at least a 2 month period.[2] Patients with CIDP generally show a positive response to corticosteroid therapy with variable long-term morbidity.

Imaging findings include focal or diffuse fusiform enlargement of nerve roots, nerve root plexi or peripheral nerves. Both CT and MRI demonstrate abnormal nerve root enhancement. T2WI reveals enlargement and abnormal hyperintense signal involving intradural and extradural spinal nerves.[5] Imaging findings do not necessarily correlate with severity of clinical disease.

Arachnoiditis:
Arachnoiditis represents a post-inflammatory disorder of the spinal meninges associated with prior spinal meningitis, myelography (particularly with oil-based or ionic water soluble contrast agents), lumbar spine surgery, intrathecal hemorrhage or spinal anesthesia.[5] While there is no distinct clinical syndrome attributable to spinal arachnoiditis, symptoms may include chronic low back pain, radicular or non-radicular lower extremity pain, as well as bowel, bladder or sexual dysfunction.[6] Clinical symptoms may be seen in 6-16% of patients following lumbar spine surgery, though radiological findings may be present without associated symptoms. Potential treatment options include intrathecal steroid injection, surgery with lysis of adhesions, spinal cord stimulation or rehabilitation.

MRI and CT myelographic findings of arachnoiditis include absence of discrete nerve roots of the cauda equina with a clumped appearance, typically involving two or more lumbar vertebral levels. Nerve roots may be diffusely adherent to the peripheral aspect of the thecal sac resulting in the so-called "empty thecal sac" sign.[7] Alternatively, nerve roots may be clumped centrally within the thecal sac forming cords or a homogenous soft tissue mass. When performing CT myelography, there may be block of intrathecal contrast with irregular contrast collections and poor filling of nerve root sleeves. MR imaging may show loculated CSF collections/cysts on T2WI and variable enhancement on post-contrast T1WI with absent, smooth or nodular enhancement involving the nerve roots and dura.[8]

Spinal meningitis:
Spinal meningitis represents infection of the spinal leptomeninges and subarachnoid space due to bacterial, viral and atypical pathogens spread via hematogenous dissemination, from an adjacent site (i.e. discitis/osteomyelitis or epidural abscess) or by direct traumatic or iatrogenic inoculation.[5] Time to symptom onset varies by the offending pathogen with bacterial etiologies generally producing symptoms within 24 hours, while atypical organisms such as Tuberculosis, Syphilis or fungal organisms may produce symptoms over several days. Symptoms include fever, chills, headache, altered mental status, convulsions, neck stiffness, paresthesias and gait dysfunction. Symptoms are generally more severe when associated with a bacterial etiology and overall, prognosis largely depends on causative pathogen, patient age and co-morbidities.[5] Treatment includes supportive care, intravenous corticosteroids to reduce inflammation/edema, and when appropriate, antibiotics aimed at specific organisms or empirically for organisms common to certain age groups.

Early imaging may be entirely normal though classically, spinal meningitis shows diffusely abnormal appearing CSF and enhancement. MR imaging findings include increased CSF signal intensity on T1WI with smooth or nodular meningeal and nerve root enhancement as well as marked enhancement of the subarachnoid space. T2WI may show areas of cord edema and intramedullary enhancement. On CT, CSF appears relatively hyperdense with abnormal enhancement of the meninges, nerve roots and within the subarachnoid space, similar to MRI.

Leptomeningeal carcinomatosis:
Leptomeningeal carcinomatosis may result from spread of primary CNS neoplasm or systemic tumors. In pediatric patients, the most common primary CNS tumors with leptomeningeal spread include medulloblastoma, germinoma, ependymoma and choroid plexus tumors. In adults, glioblastoma multiforme, anaplastic astrocytoma and ependymomas are the most common primary CNS sources. Systemic tumors may metastasize to the spine via hematogenous spread or direct extension to the subarachnoid space, most commonly due to breast or lung primaries, as well as melanoma, lymphoma and leukemia. Patients typically present with headache, cranial nerve symptoms, pain and radiculopathy. Lumbar puncture with CSF cytology is the most sensitive method of detecting leptomeningeal carcinomatosis.[3] Prognosis is poor, and treatment generally consists of intrathecal chemotherapy and radiation.

Imaging findings of leptomeningeal carcinomatosis include smooth or nodular (more

common) enhancement along any level of the spinal cord or nerve roots. Enhancement patterns consist of a solitary focal mass, diffuse smooth enhancement of the cord and nerve roots, "rope-like" thickening of cauda equina and multifocal nodular enhancement.[5] In the case of CSF dissemination due to primary CNS tumors, imaging should be performed prior to tumor resection as redistribution of blood products into the spinal subarachnoid space could be misinterpreted as tumor spread.

Diagnosis

Guillain-Barré syndrome

Summary

Numerous pathological entities can result in enlargement and/or enhancement of spinal nerve roots. Though the imaging is often nonspecific, when taken in context of the patient's age, clinical presentation and CSF analysis, a definitive diagnosis is often possible. When present, certain features of nerve root enhancement can help limit the differential diagnosis, including preferential smooth enhancement of ventral (motor) nerve roots in Gullain-Barré syndrome versus more diffuse irregular nerve root enhancement in the setting of arachnoiditis or neoplastic/granulomatous diseases. MRI is the primary imaging modality of choice when evaluating for spinal cord or nerve root enhancement and recognition of the varying patterns of enhancement will aid in differential diagnosis, evaluating the burden of disease and for assessing treatment response.

References

1. Given CA, Santos, C.C., and Durden, D.D. Intracranial and Spinal MR Imaging Findings Associated with Krabbe's Disease: Case Report. AJNR 2001;22:1782-5.
2. Lewis RA. Chronic inflammatory demyelinating polyneuropathy. Neurol Clin 2007;25:71-87.
3. Atlas S, ed. Spinal Infection and Inflammatory Disorders. 4th ed. Philadelphia: Lippincott Williams & Wilkins; 2009.
4. DeSanto J, Ross JS. Spine infection/inflammation. Radiol Clin North Am 2011;49:105-27.
5. Ross JS, et al., ed. Diagnostic Imaigng: Spine. 1st ed. Salt Lake City: Amirsys; 2005.
6. Petty PG, Hudgson, P., Hare, W.S.C. Symptomatic lumbar spinal arachnoiditis: fact or fallacy? Journal of Clinical Neuroscience 2000;7:395-9.
7. Ross J, Masaryk, TJ, Modic, MT, Delamater, R, Bohlman, H, Wilbur, G, Kaufman, B. MR Imaging of Lumbar Arachnoiditis. AJR 1987:1025-32.
8. Johnson CE, Sze, G. Benign Lumbar Arachnoiditis: MR Imaging with Gadopentetate Dimeglumine. AJNR 1990;11:763-70.

JAOCR at the Viewbox

Marguerite M. Caré, M.D.

Division of Neuroradiology, Cincinnati Children's Hospital Medical Center, Cincinnati, OH

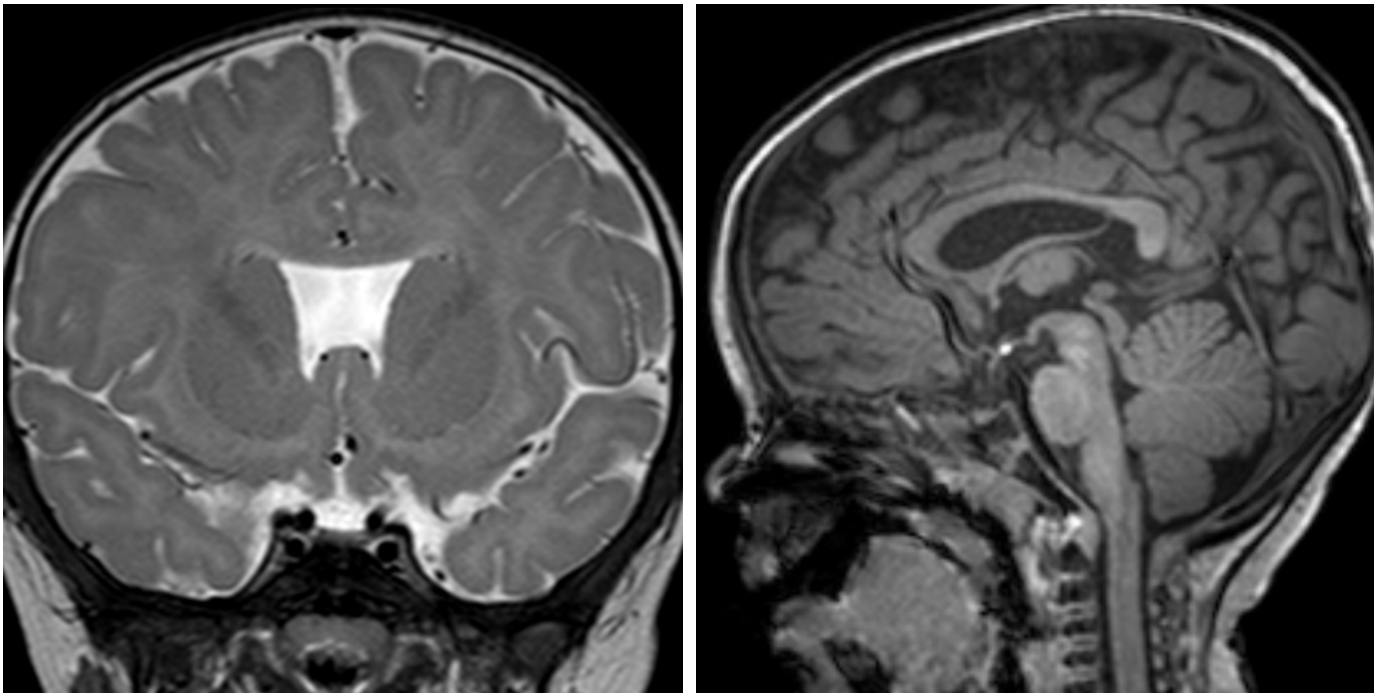

Absent septum pellucidum with ectopic posterior pituitary:

Why was this patient referred for imaging from an ophthalmologist? The coronal T2 image demonstrates absence of the septum pellucidum causing the unusual configuration of the lateral ventricles with a flattened superior margin and pointed inferior frontal horns. The sagittal T1 image demonstrates the T1 hyperintense focus of the posterior pituitary in an ectopic location near the hypothalamic region instead of the normal sellar location. The pituitary infundibulum is thin. When these findings are present, the imaging should be reviewed for additional findings of septo-optic dysplasia (SOD). Septo-optic dysplasia classically presents with midline structural abnormalities of the brain including optic nerve hypoplasia, absence or hypoplasia of the septum pellucidum, and hypothalamic-pituitary abnormalities. In patients with SOD, optic nerve hypoplasia is bilateral in almost two-thirds of patients. Almost half of patients will have pituitary insufficiency with imaging findings including an ectopic posterior pituitary, small pituitary gland, and thin or absent pituitary infundibulum. Additional brain malformations such as cortical malformations and schizencephaly are common. When these additional malformations are present, the disorder is sometimes referred to as septo-optic dysplasia plus.

JAOCR at the Viewbox

Stefan Hamelin, M.D., William T. O'Brien, Sr., D.O.

Department of Diagnostic Imaging, Wilford Hall Ambulatory Surgical Center, San Antonio, TX

Cavernous sinus invasion with cranial nerve palsy:

Can you tell how this patient presented clinically? This axial T2 image demonstrates a large hypointense suprasellar mass which is eccentric to the right and encroaches on the cavernous segment of the right internal carotid artery. When presented with a suprasellar mass, determining whether or not there is cavernous sinus invasion is critical in terms of management. Cavernous sinus invasion is suspected when a mass encircles two-thirds or results in narrowing of the cavernous internal carotid artery. With cavernous sinus invasion, patients may present with cranial nerve palsies. From superior to inferior, cranial nerves III, IV, V1, and V2 travel along the lateral wall of the cavernous sinus. Cranial nerve VI is located medially within the cavernous sinus, making it more vulnerable in cases of cavernous sinus invasion. With CN VI (abducens) palsy, the lateral rectus muscle cannot rotate the globe laterally; thus, the affected globe is medially rotated. This is a unique case in which the lateral rectus palsy can be seen on imaging with the right globe medially deviated, resulting in a disconjugate gaze.

JAOCR at the Viewbox

Anthony I. Zarka, D.O.

Department of Diagnostic Imaging, Wilford Hall Ambulatory Surgical Center, San Antonio, TX

Aggressive vertebral body hemangioma:

This teenage boy presented with chronic progressive neurological deficits involving the lower extremities. A contrast enhanced CT shows an expanded, rarefied T3 vertebral body with disruption of the posterior cortex and an associated enhancing epidural mass. The sagittal image reveals exaggerated vertical bony striations within the affected vertebral body. The axial image demonstrates a bilobed appearance to the epidural portion of the mass with severe central canal stenosis and presumed cord compression. Commonly invoked radiology descriptions of this “classic” bony lesion on axial CT include a "corduroy", "polka dot", and "salt-and-pepper" appearance.

The majority of vertebral body hemangiomas are asymptomatic and incidental. Rarely, lesions may enlarge and cause pain or neurological deficits due to spinal cord compression, vertebral body or arch expansion, or pathologic fracture. Additional important findings include paravertebral soft tissue extension and enlarged vasculature. Vertebral hemangiomas are highly vascular and are commonly associated with a high volume of intraoperative blood loss. Consequently, there is a preference to perform preoperative embolization prior to surgical intervention. The bilobed posterior epidural protrusion is a unique feature. The reason for this appearance is the protruding hemangiomatous masses are tethered centrally by the posterior longitudinal ligament and midline sagittal septum.